CHEMICAL ENGINEERING SCIENCE
GENIE CHIMIQUE

VOL. 5 JULY 1956 No. 4

The vapour pressure-temperature relationship of liquids

J. CORNELISSEN and H. I. WATERMAN

The Institute of Chemical Engineering, The University, Delft

Abstract—The formula $\log P = \frac{A}{T^x} + B$ is applied to pure liquid hydrocarbons, *viz.* the series of the homologous compounds of the n-paraffins, olefins, n-alkylcyclopentanes, n-alkylcyclohexanes, n-alkylbenzenes; liquid isomers of n-hexane, n-heptane, n-octane and n-nonane; cis and trans derivatives of cyclohexane and cyclopentane.

Other liquids also obey the equation, *e.g.* sulphur containing organic compounds such as sulphides, mercaptans, thiophene. For all these substances the value of x appears to be $1{\cdot}5 \pm 0{\cdot}2$.

Good results are obtained when the equation is applied to water. For the temperature range of 50°C to 374°C (the critical point of water) the value of x appears to be 1·2. Other liquids to which application of the formula gives satisfactory results are intermediates in the preparation of silicones, besides mixtures of water and sulphuric acid.

Résumé—Les auteurs appliquent la formule : $\log P = \frac{A}{T^x} + B$ aux hydrocarbures liquides purs : les séries des composés homologues des n-paraffines, oléfines, n-alkylcyclopentanes, n-alkylcyclohexanes, n-alkylbenzènes ; les isomères liquides des n-hexanes, n-heptanes, n-octanes et n-nonane ; les dérivés cis et trans du cyclohexane et du cyclopentane.

D'autres liquides obéissent aussi à cette équation : dérivés soufrés contenant des composés organiques tels que sulfures, mercaptans, thiophene. Pour toutes ces substances, x est égal à $1{\cdot}5 + 0{\cdot}2$.

Ils obtiennent de bons résultats avec l'eau. Dans l'intervalle de température 50°C à 473°C (point critique de l'eau), x est égal à 1·2. La formule donne également de bons résultats pour des composés intermédiares dans la préparation des silicones et aussi pour les mélanges eau-acide sulfurique.

INTRODUCTION

In a previous communication [1] the usefulness was discussed of the formula

$$\log \nu = \frac{A}{T^x} + B \qquad (1)$$

indicating the relationship between viscosity and temperature.

ν = kinematic viscosity in cs, T = absolute temperature, and A, B and x are constants.

The relationship is a simple exponential function. It rendered possible the classification and prediction of the results of the measurement of viscosity values for various single liquid compounds, and liquid mixtures of solid substances and liquids.

An analogous equation is valid for the classification of substances by means of other physical constants. In this paper the authors consider the dependence of the vapour pressure P on the temperature T, given by the equation

$$\log P = \frac{A}{T^x} + B. \qquad (2)$$

A, B and x are constants. As will be seen below in the discussion of the literature, this formula has already been proposed by HENGLEIN. The authors did not carry out vapour-pressure measurements as they did with the viscosity. In

the literature however a large number of reliable vapour-pressure data is available.

Many investigators tried to indicate the relationship between vapour pressure and temperature according to experimental data. The earliest vapour-pressure formula was proposed by DALTON [2]

$$\log P = a + b\,T \tag{3}$$

where a and b are constants.

The formula was replaced by more satisfactory formulae, such as that proposed by ANTOINE [3]

$$\log P = A + \frac{B}{T + C} \tag{4}$$

A, B and C are constants, B generally being negative.

Other investigators extensively used this formula, *e.g.* SCHMIDT [4], and CALINGAERT and DAVIS [5], and recently F. ROSSINI c.s., A.P.I. Research Project 44, Table *k* [13]. CALINGAERT and DAVIS classified several groups of compounds (metallic elements, acids, alcohols, hydrocarbons) by means of equation (4), taking for C the value $C = 230$.

The best-known, but not generally applicable, equation is that of CLAUSIUS-CLAPEYRON

$$\log P = \frac{A}{T} + B \tag{5}$$

A and B are constants. Other well-known formulae are those of RANKINE [6] and KIRCHHOFF [7]

$$\log P = A + \frac{B}{T} + C \log T, \tag{6}$$

and NERNST [9]

$$\log P = A + \frac{B}{T} + C \log T + DT. \tag{7}$$

The equations (6), (5) and (7) may be derived as follows from the CLAPEYRON equation

$$\frac{dP}{dT} = \frac{Q_v}{T \cdot \Delta V} \tag{8}$$

Q_v = molecular heat of vaporization, $\Delta V = V_g - V_1$, V_g = molecular volume of the gaseous phase, and V_1 = molecular volume of the corresponding liquid phase.

The compressibility factors Z_g and Z_1 are introduced as follows:

$$Z_g = \frac{PV_g}{RT} \text{ and } Z_1 = \frac{PV_1}{RT}. \tag{9}$$

From these it follows

$$\Delta V = V_g - V_1 = \frac{RT}{P} Z_g - \frac{RT}{P} Z_1 = \frac{RT}{P}(Z_g - Z_1)$$

$$\Delta V = \frac{RT}{P} \cdot \Delta Z. \tag{10}$$

Substitution of equation (10) in the Clapeyron equation (8) gives

$$\frac{dP}{dT} = \frac{Q_v}{T \cdot \frac{RT}{P} = \cdot \Delta Z}$$

or

$$\frac{dP}{P} = \frac{Q_v}{\Delta Z} \cdot \frac{1}{RT^2}\,dT \tag{11}$$

The expression $\frac{Q_v}{\Delta Z}$ is only feebly dependent on the temperature, and may be described as a power series in T

$$\frac{Q}{\Delta Z} = Q_0 + AT + BT^2 + CT^3 + \ldots$$

Substituting this expression in (11) gives

$$\frac{dP}{P} = \left(\frac{Q_0}{RT^2} + \frac{A}{RT} + \frac{B}{R} + \frac{C}{R} \ldots.\right) dT.$$

Integration gives the following relation between vapour pressure and temperature

$$\log P = \text{constant} - \frac{Q_0'}{RT} + \frac{A'}{R} \log T + \frac{B'}{R}\,T + \frac{C'}{2R}\,T^2 + \ldots \tag{12}$$

By omitting the third and further terms in (12) the Clausius-Clapeyron equation is obtained. By omitting the fourth and higher terms the Rankine-Kirchhoff equation is obtained. By omitting the fifth and higher terms the Nernst equation is obtained.

It must be noticed that these equations have not been derived in this way by the authors who originally proposed them; but the present authors consider the given derivation of the

VOL. 5 1956

Table 1

Compound	x	$P_{pred.}$ 85°C (185°F)	$P_{exp.}$ 85°C (185°F)	ΔP %	$P_{pred.}$ 110°C (230°F)	$P_{exp.}$ 110°C (230°F)	ΔP %	$P_{pred.}$ 135°C (275°F)	$P_{exp.}$ 135°C (275°F)	ΔP %	$P_{pred.}$ 160°C (320°F)	$P_{exp.}$ 160°C (320°F)	ΔP %	$P_{pred.}$ 185°C (365°F)	$P_{exp.}$ 185°C (365°F)	ΔP %
n-propylbenzene	1·42	1·358	1·359	−0·1	3·452	3·432	0·6	7·604	7·570	0·4	15·06	14·99	0·5	27·23	27·22	0·0
n-butylbenzene	1·43	0·572	0·575	−0·5	1·592	1·592	0·0	3·82	3·789	0·8	8·07	8·00	0·9	15·31	15·33	−0·1
n-pentylbenzene	1·70				0·7607	0·77	−1·3	1·968	1·96	0·4	4·446	4·39	1·3	8·89	8·84	0·6
n-hexylbenzene	1·62							1·016	1·00	1·6	2·45	2·45	0·0	5·19	5·19	0·0
n-heptylbenzene	1·49										1·34	1·35	−0·6	3·03	3·03	0·0
n-octylbenzene	1·49										0·762	0·76	0·3	1·807	1·80	0·4
n-nonylbenzene	1·53													1·07	1·06	0·9
n-decylbenzene	1·69													0·646	0·644	0·3
n-undecylbenzene	1·55															
n-dodecylbenzene	1·62															
n-tridecylbenzene	1·67															

Compound	x	$P_{pred.}$ 210°C (410°F)	$P_{exp.}$ 210°C (410°F)	ΔP %	$P_{pred.}$ 235°C (455°F)	$P_{exp.}$ 235°C (455°F)	ΔP %	$P_{pred.}$ 260°C (500°F)	$P_{exp.}$ 260°C (500°F)	ΔP %	$P_{pred.}$ 285°C (545°F)	$P_{exp.}$ 285°C (545°F)	ΔP %	$P_{pred.}$ 310°C (590°F)	$P_{exp.}$ 310°C (590°F)	ΔP %
n-propylbenzene	1·42															
n-butylbenzene	1·43	26·92	27·15	−0·8												
n-pentylbenzene	1·70	16·33	16·3	0·2	28·5	28·1	1·4									
n-hexylbenzene	1·62	0·991	10·03	−1·2	17·87	17·9	−0·2	30·06	30·0	0·2						
n-heptylbenzene	1·49	6·14	6·14	0·0	11·54	11·44	0·9	19·9	19·9	0·0						
n-octylbenzene	1·49	3·82	3·83	−0·3	7·38	7·43	−0·7	13·42	13·34	0·6	22·6	22·5	0·4			
n-nonylbenzene	1·53	2·36	2·38	−0·9	4·79	4·82	−0·6	8·91	8·99	−0·9	15·60	15·65	−0·3	25·5	25·7	−0·8
n-decylbenzene	1·69	1·500	1·517	−1·1	3·192	3·207	−0·5	6·180	6·203	−0·4	11·27	11·14	1·2	18·97	18·80	0·9
n-undecylbenzene	1·55	0·959	0·96	−0·1	2·128	2·12	0·4	4·285	4·27	0·4	7·925	7·92	0·1	13·71	13·75	−0·3
n-dodecylbenzene	1·62	0·594	0·60	−1·0	1·393	1·41	−1·2	2·91	2·94	−1·0	5·66	5·66	0·0	10·09	10·12	−0·3
n-tridecylbenzene	1·67				0·938	0·93	0·9	2·03	2·04	−0·5	4·055	4·06	−0·1	7·45	7·49	−0·5

P in p.s.i.a.

Table 2

Compound	x	$P_{pred.}$ 10°C (50°F)	$P_{exp.}$ 10°C (50°F)	ΔP %	$P_{pred.}$ 35°C (95°F)	$P_{exp.}$ 35°C (95°F)	ΔP %	$P_{pred.}$ 60°C (140°F)	$P_{exp.}$ 60°C (140°F)	ΔP %	$P_{pred.}$ 85°C (185°F)	$P_{exp.}$ 85°C (185°F)	ΔP %
thiophene	1·38	0·720	0·724	−0·6	2·438	2·447	−0·5	6·61	6·56	0·8	15·03	15·08	−0·3
3-thiaheptane $C_2H_5SC_4H_9$	1·44							0·757	0·76	−0·4	2·19	2·19	0·0
2-methylthiacyclohexane	1·36							0·628	0·63	−0·3	1·79	1·78	0·6
1, cis-2-dimethylcyclohexane	1·37				0·469	0·471	−0·4	1·479	1·468	0·8	3·802	3·791	0·3
1, trans-2-dimethylcyclohexane	1·35				0·621	0·619	0·3	1·879	1·858	1·1	4·667	4·653	0·3

Compound	x	$P_{pred.}$ 110°C (230°F)	$P_{exp.}$ 110°C (230°F)	ΔP %	$P_{pred.}$ 135°C (275°F)	$P_{exp.}$ 135°C (275°F)	ΔP %	$P_{pred.}$ 160°C (320°F)	$P_{exp.}$ 160°C (320°F)	ΔP %
thiophene	1·38	30·27	30·56	−0·9						
3-thiaheptane $C_2H_5SC_4H_9$	1·44	5·36	5·33	0·6	11·35	11·40	−0·4	21·9	22·0	−0·5
2-methylthiacyclohexane	1·36	4·34	4·28	1·4	9·14	9·10	0·4	17·50	17·46	0·2
1, cis-2-dimethylcyclohexane	1·37	8·531	8·464	0·8	16·71	16·85	−0·9			
1, trans-2-dimethylcyclohexane	1·35	10·21	10·14	0·7	19·59	19·79	−1·0			

P in p.s.i.a.

Table 3. Water; P in mm Hg.

Temp. °C	$P_{pred.}$	$P_{exp.}$	ΔP %
50	92·9	92·51	0·4
60	148·3	149·38	− 0·8
85	431·5	433·6	− 0·5
110	1062	1074·6	− 1·2
135	2334	2347	− 0·6
160	4656	4636	0·4
185	8492	8424	0·8
210	14450	14305	1·0
235	23020	22968	0·2
260	35560	35190	1·0
285	52480	51840	1·2
310	74820	74020	1·1
335	103000	102880	0·1
360	138400	139900	− 1·1
374	163300	165470	− 1·3

equations a convenient way to find a connection between them. By the way, the derivation has been proposed by THOMSON [11].

The Rankine-Kirchhoff equation has also been derived by DE WIJS [8] who used the Clapeyron equation (8) besides the experimental equation

$$Q_v = k\,(T_k - T)^m \qquad (13)$$

Q_v = heat of vaporization, k and m are constants, T_k = critical temperature °K, and T = absolute temperature °K.

In the foregoing an assumption was made regarding the temperature dependence of the expression $\frac{Q_v}{\Delta Z}$. This assumption is not absolutely exact. Therefore all the formulae derived by means of the said assumption lack a theoretical base, and in this respect the formulae (5), (6) and (7) are completely comparable with empirically established formulae such as (2) and (4).*

One equation deserves special attention, *viz.* the equation (2) already proposed by HENGLEIN [12]

$$\log P = \frac{A}{T^x} + B \qquad (2)$$

* Other experimental formulae have been proposed but will not be discussed here. A survey of these equations can be found in the French literature [10], and is also given by THOMSON [11].

VOL. 5 1956

Table 4

Mixture	x	$P_{pred.}$ 10°C (50°F)	$P_{exp.}$ 10°C (50°F)	ΔP %	$P_{pred.}$ 35°C (95°F)	$P_{exp.}$ 35°C (95°F)	ΔP %	$P_{pred.}$ 60°C (140°F)	$P_{exp.}$ 60°C (140°F)	ΔP %	$P_{pred.}$ 85°C (185°F)	$P_{exp.}$ 85°C (185°F)	ΔP %	$P_{pred.}$ 110°C (230°F)	$P_{exp.}$ 110°C (230°F)	ΔP %
20% H_2SO_4–80% H_2O	1·30	8·09	8·05	0·5	37·4	37·2	0·5	132·4	133	−0·5	386·4	385	0·4	692	679	1·9
40% H_2SO_4–60% H_2O	1·11	5·28	5·22	1·1	24·1	24·3	−0·8	85·7	87·2	−1·8	259	261	−0·8	267	260	2·7
60% H_2SO_4–40% H_2O	1·03	1·47	1·46	0·7	7·41	7·39	0·3	29·0	29·3	−1·0	94·2	94·3	−0·2	23·0	22·5	2·2
80% H_2SO_4–20% H_2O	0·96				0·268	0·265	1·1	1·45	1·47	−1·4	6·31	6·35	−0·6	0·446	0·437	2·1
95% H_2SO_4– 5% H_2O	0·97															

Mixture	x	$P_{pred.}$ 135°C (275°F)	$P_{exp.}$ 135°C (275°F)	ΔP %	$P_{pred.}$ 160°C (320°F)	$P_{exp.}$ 160°C (320°F)	ΔP %	$P_{pred.}$ 185°C (365°F)	$P_{exp.}$ 185°C (365°F)	ΔP %	$P_{pred.}$ 210°C (410°F)	$P_{exp.}$ 210°C (410°F)	ΔP %	$P_{pred.}$ 235°C (455°F)	$P_{exp.}$ 235°C (455°F)	ΔP %
20% H_2SO_4–80% H_2O	1·30															
40% H_2SO_4–60% H_2O	1·11															
60% H_2SO_4–40% H_2O	1·03	650	647	0·5												
80% H_2SO_4–20% H_2O	0·96	70·3	69·0	1·9	186	188	−1·1	44·9	45·0	−0·2						
95% H_2SO_4– 5% H_2O	0·97	1·88	1·87	0·5	6·58	6·47	1·7	20·1	20·1	−0·5	55·5	55·0	0·9	136	137	−0·7

P in mm Hg

Table 5

Temp. °C	*Bistrichlorosilylethane* $P_{pred.}$	$P_{exp.}$	ΔP %	*Temp.* °C	*Diphenyldichlorosilane* $P_{pred.}$	$P_{exp.}$	ΔP %	*Temp.* °C	*Ethyldichlorosilane* $P_{pred.}$	$P_{exp.}$	ΔP %
91·2	18·66	18·5	0·9	192·1	37·5	37·4	0·3	6·0	50·8	50·0	1·6
114·7	48·1	48·2	− 0·2	210·7	69·2	69·8	− 0·9	21·3	103·0	103·9	− 0·9
147·1	152·8	154·2	− 0·9	235·6	146·2	147·1	− 0·6	31·1	156·3	155·4	0·6
159·9	233·9	231·0	1·3	260·2	279·9	218·3	− 0·5	35·5	186·6	187·5	− 0·5
				281·2	462·4	462·6	0·0	45·6	276·1	274·3	0·7
								49·3	316·2	315·6	0·2
								53·2	362·2	363·1	− 0·3
								61·4	480·8	482·5	− 0·4
								73·1	709·6	703·2	0·9
	$x = 0·74$				$x = 1·65$				$x = 1·06$		

P in mm Hg

The authors give preference to this equation for reasons which will be discussed in the following pages.

Equation (2)

$$\log P = \frac{A}{T^{\circ}} + B \qquad (2)$$

is applied to many substances represented in the figures 2 to 18.

Table 6. 1,1-*dimethylcyclopentane*; *P in mm Hg.*

Temp. °C	$P_{calc.}$	$P_{exp.}$	ΔP %
88·736	780·03	779·99	+ 0·005
88·227	768·37	768·49	− 0·016
87·647	755·55	755·59	− 0·005
87·137	744·13	744·40	− 0·036
86·585	732·32	732·40	− 0·011
81·470	628·10	628·20	− 0·016
74·228	501·03	500·99	+ 0·008
67·558	402·67	402·72	− 0·012
61·312	325·11	325·17	− 0·018
50·257	217·38	217·36	+ 0·009
44·815	176·10	176·08	+ 0·011
40·744	149·57	149·60	− 0·020
36·361	124·78	124·81	− 0·024
32·069	103·88	103·81	+ 0·067
28·300	87·948	87·92	+ 0·032
25·476	77·416	77·47	− 0·070
22·527	67·520	67·43	+ 0·134
19·262	57·827	57·72	+ 0·185
15·498	48·120	48·12	0·000

The first group (Figs. 1 to 8) is that of some series of homologous hydrocarbons, *viz.*

n-alkanes	Figs. 1 and 2
n-alkylcyclohexanes	Figs. 3 and 7
n-alkylcyclopentanes	Figs. 4 and 8
n-alkylbenzenes	Fig. 5
n-alkenes	Fig. 6

The data used were taken from the American Petroleum Institute Research Project 44 [13].

Fig. 1 is given as an illustration of the deviation from the straight line if the formula

$$\log P = \frac{A}{T} + B \qquad (5)$$

is used instead of equation (2).

The value of x in equation (2) for the homologous series appears to be $1{\cdot}5 \pm 0{\cdot}2$. For all the considered members of these series the value of $x = 1{\cdot}5$ was used to construct the diagrams $\log P = f\left(\frac{1}{T^{x}}\right)$. An example of the predicted values of P from the diagram $\log P = f\left(\frac{1}{T^{1{\cdot}5}}\right)$ is given in Table 1 for the homologous series of n-alkylbenzenes.

It may be concluded that the value of P for the substances in question can be predicted from the diagram $\log P = f\left(\frac{1}{T^{1{\cdot}5}}\right)$ with a maximum error of 1·5%, but generally with an error not larger than 1·0%.

The second group includes other organic liquids, *viz.*

cis-trans isomers of cyclohexane derivatives	Fig. 7
cis-trans isomers of cyclopentane derivatives	Fig. 8
isomers of hexane	Fig. 9
isomers of heptane	Fig. 9
isomers of octane	Figs. 9 and 10
isomers of nonane	Fig. 11

besides sulphur-containing organic compounds, *viz.*

thiophene	Fig. 10
sulphides (aliphatic and cyclic)	Fig. 12

For all these substances the value of x appeared to be also $1{\cdot}5 \pm 0{\cdot}2$. Diagrams representing $\log P = f\left(\frac{1}{T^{1{\cdot}5}}\right)$ were constructed, and from these diagrams it is possible to predict values of P ar various temperatures T. Examples are given in Table 2. Deviations of the predicted values of P from the experimental values rarely exceed 1·0%. Data have again been taken from the American Petroleum Institute Research Project 44 [13].

A third group of substances comprises water and its mixtures with sulphuric acid, *viz.*

Water	Fig. 13
80% water – 20% H_2SO_4	Fig. 14
60% water – 40% H_2SO_4	Fig. 15
40% water – 60% H_2SO_4	Fig. 15
20% water – 80% H_2SO_4	Fig. 15
5% water – 95% H_2SO_4	Fig. 15

Water has been examined over the whole temperature range from 50°C to the critical temperature (374°C), and accurate calculations show that the value of x varies from 1·3 in the lower region to 1·1 in the higher region. The mean

VOL.
5
1956

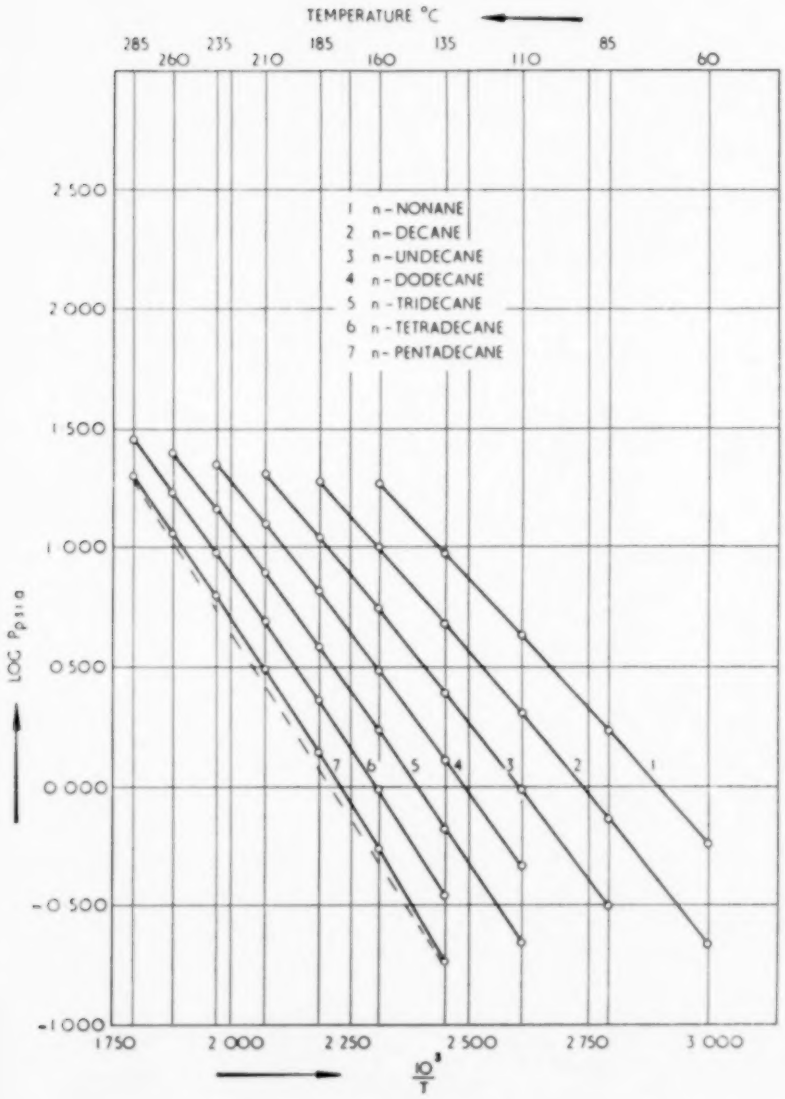

FIG. 1. $\log P - \frac{1}{T}$ diagram for some members of the series of n-alkanes.

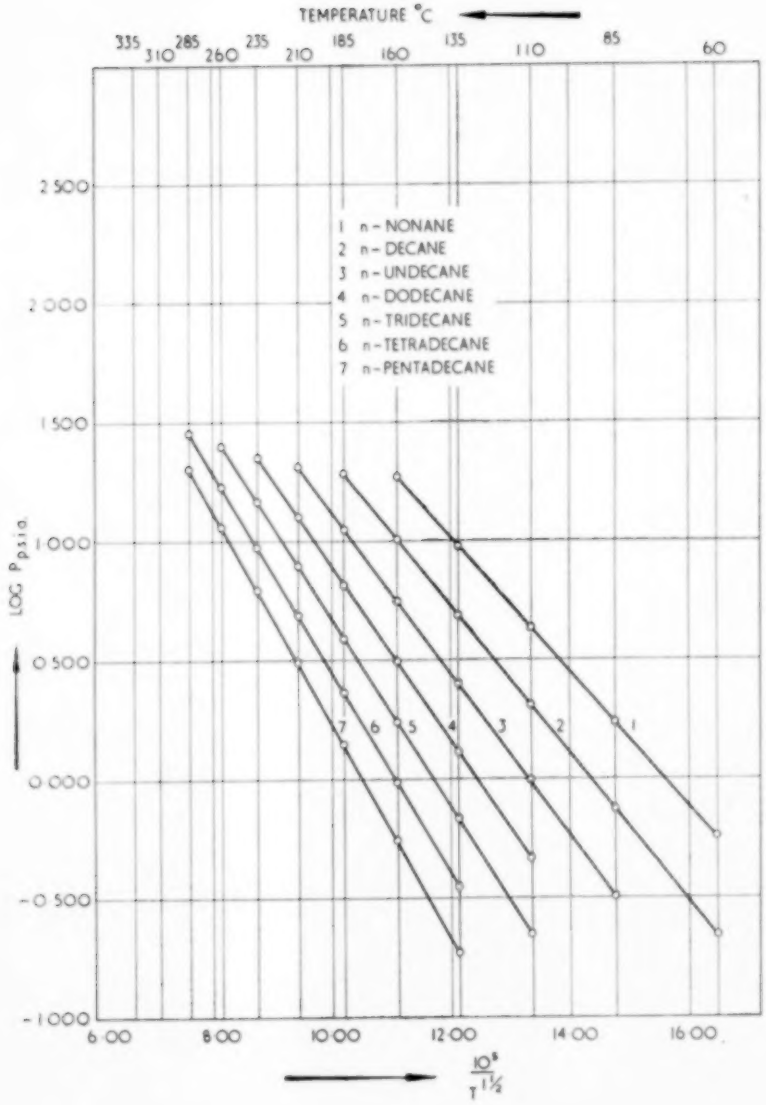

FIG. 2. $\log P - \frac{1}{T^{1\cdot5}}$ diagram for some members of the series of n-alkanes.

VOL. 5 1956

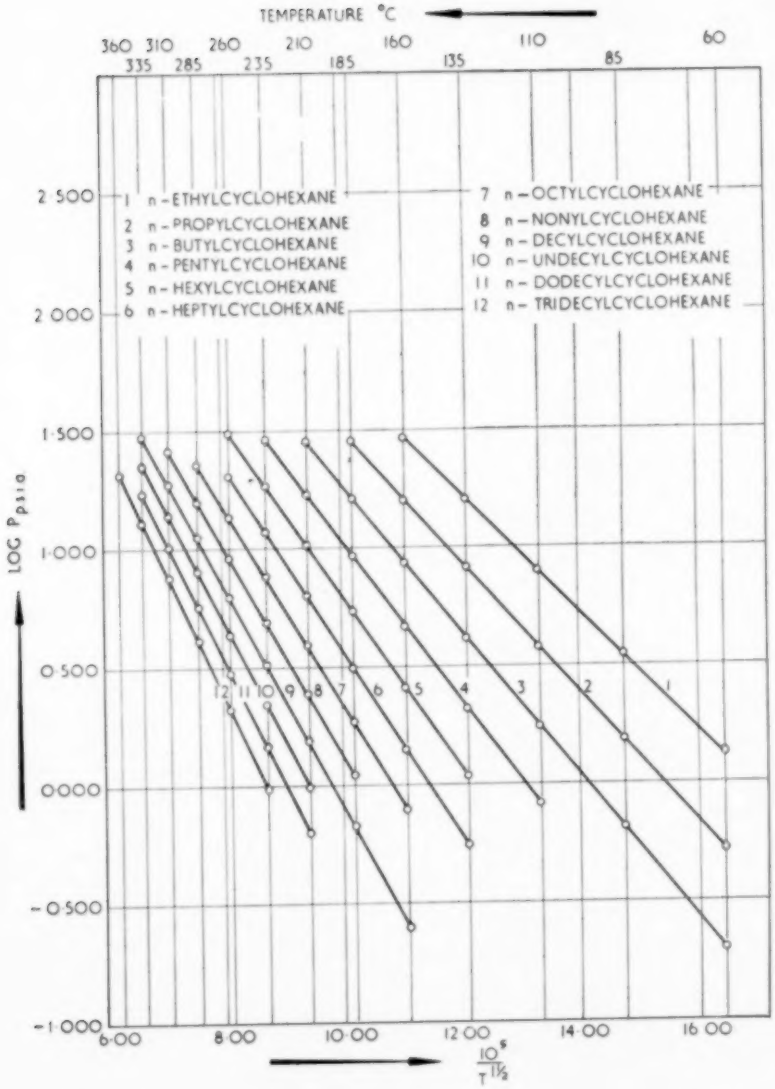

FIG. 3. $\log P - \frac{1}{T^{1\cdot5}}$ diagram for some members of the series of n-alkylcyclohexanes.

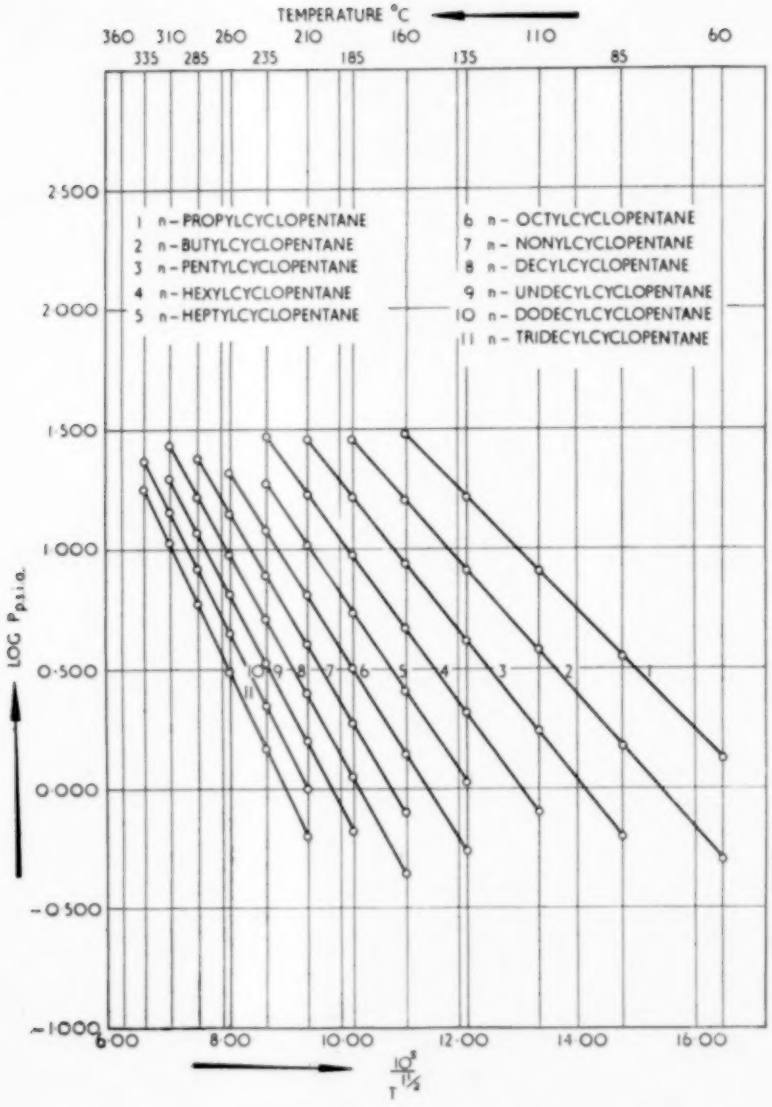

FIG. 4. $\log P - \frac{1}{T^{1\cdot5}}$ diagram for some members of the series of n-alkylcyclopentanes.

VOL. 5 1956

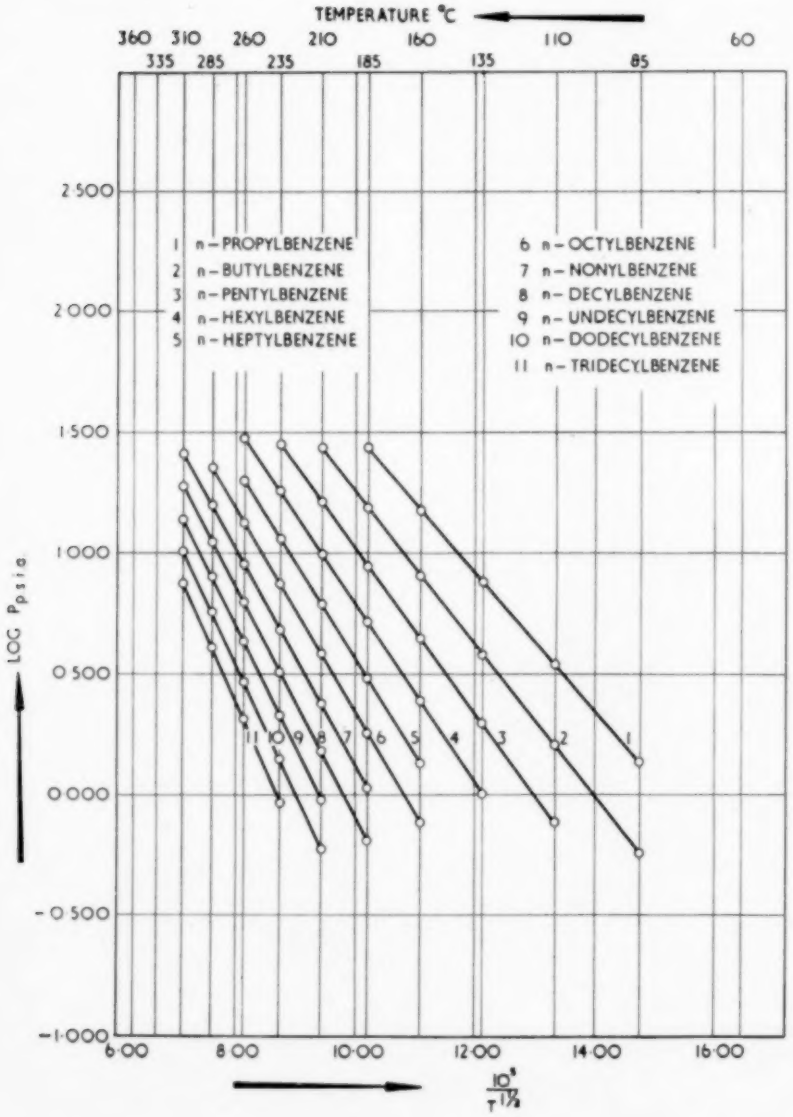

FIG. 5. $\log P - \frac{1}{T^{1.5}}$ diagram for some members of the series of n-alkylbenzenes.

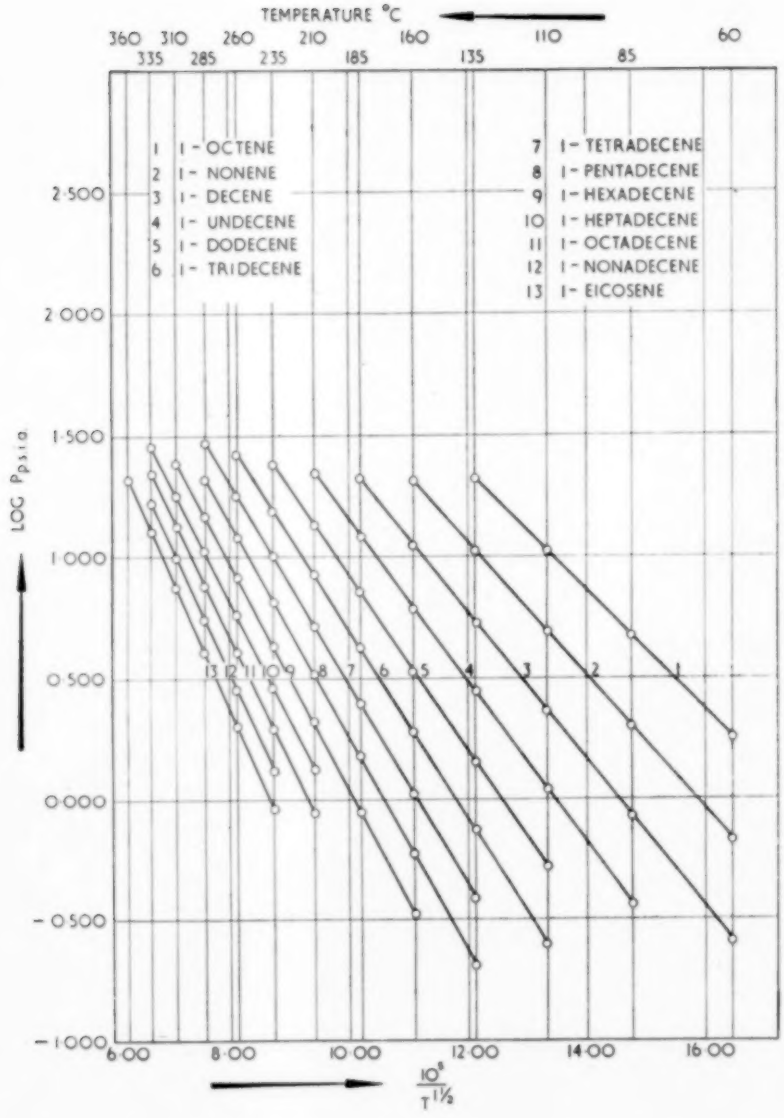

FIG. 6. $\log P - \frac{1}{T^{1\cdot5}}$ diagram for some members of the series of n-alkenes.

VOL. 5 1956

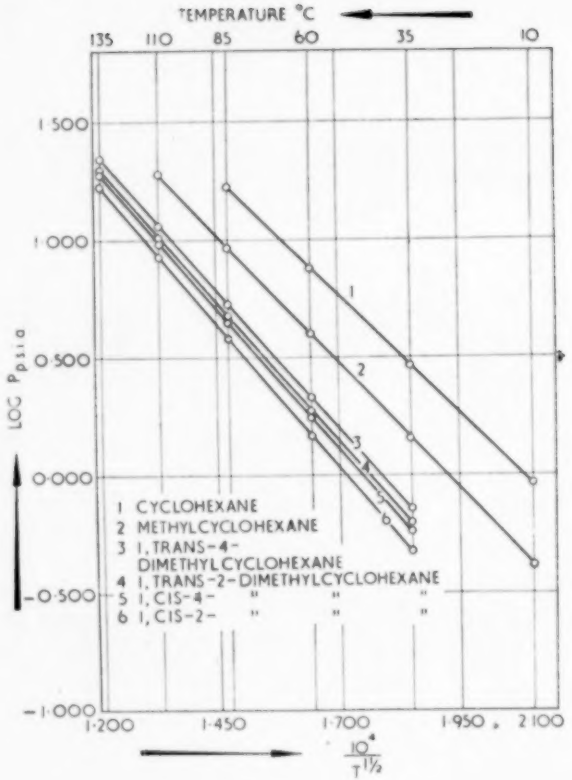

FIG. 7. $\log P - \frac{1}{T^{1\cdot5}}$ diagram for some cis-trans isomers of cyclohexane derivatives, cyclohexane itself and methylcyclohexane.

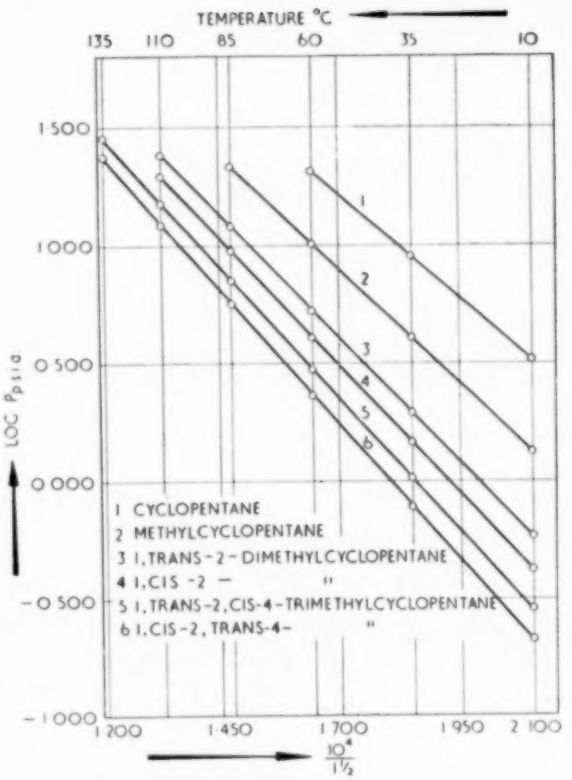

FIG. 8. $\log P - \frac{1}{T^{1\cdot5}}$ diagram for some cis-trans isomers of cyclopentane derivatives, cyclopentane iteslf and methylcyclopentane.

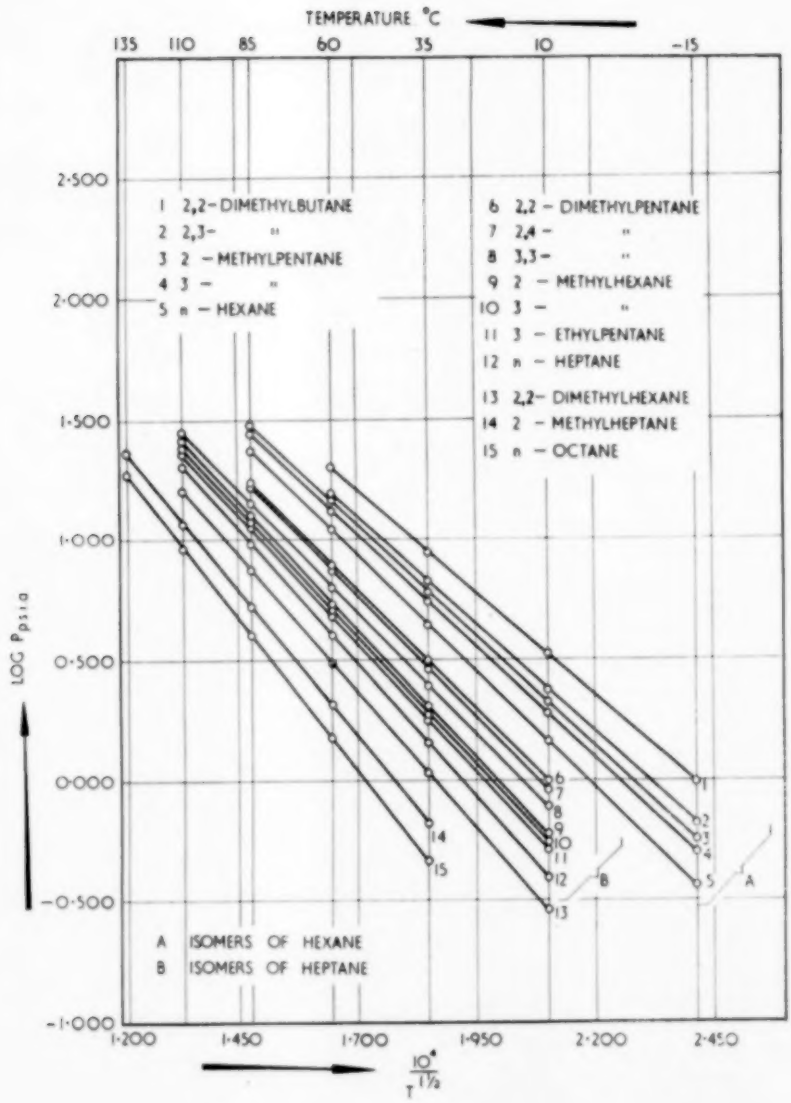

FIG. 9. $\log P - \frac{1}{T^{1\cdot5}}$ for diagram some isomers of hexane, heptane and octane.

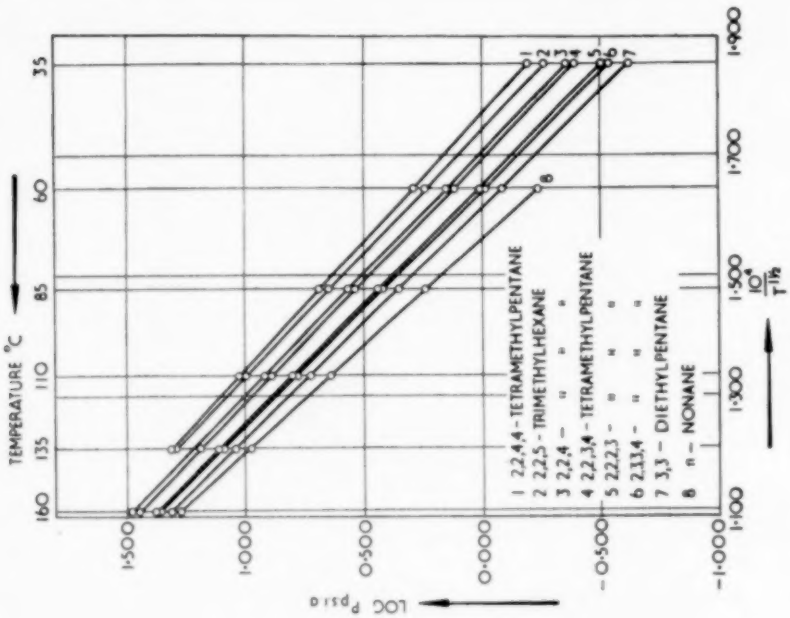

FIG. 11. $\log P - \frac{1}{T^{1\cdot5}}$ diagram for some isomers of nonane

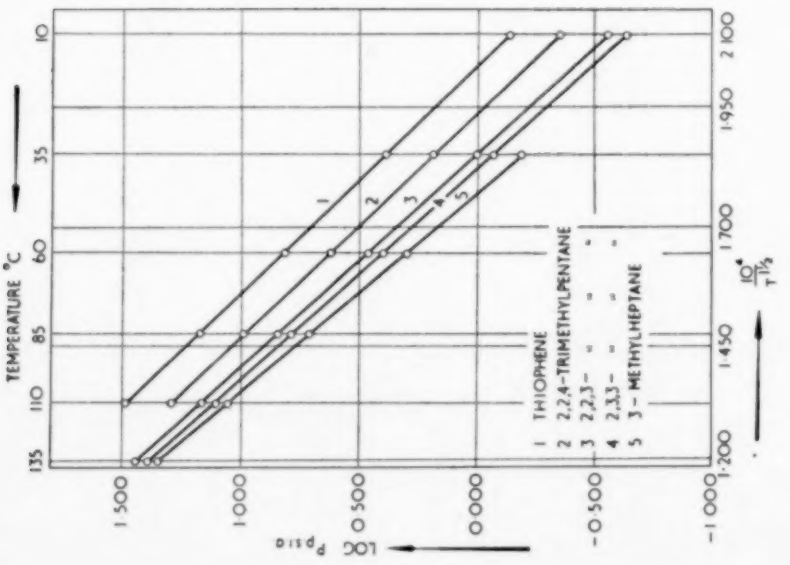

FIG. 10. $\log P - \frac{1}{T^{1\cdot5}}$ diagram for thiophene and some isomers of octane.

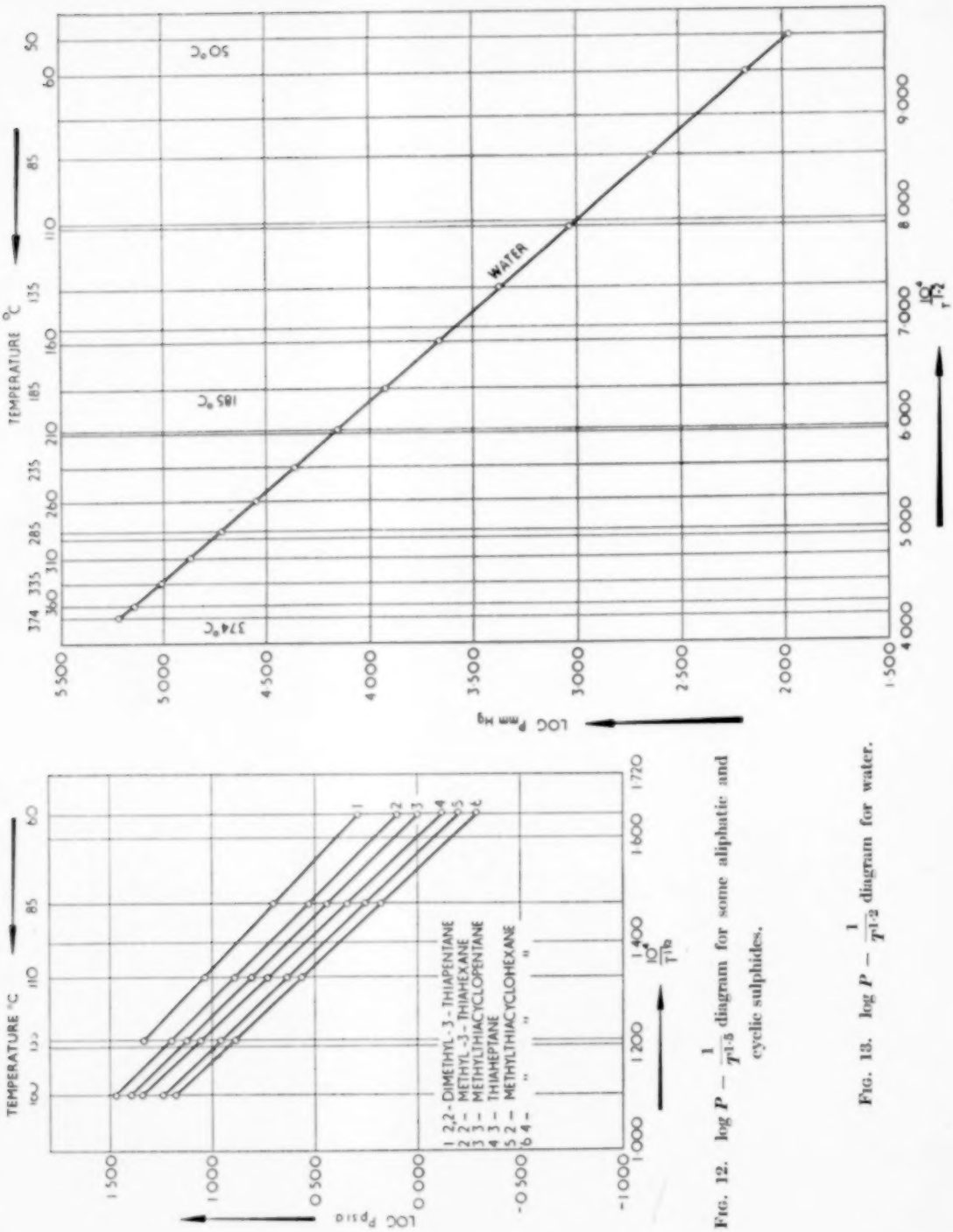

FIG. 12. $\log P - \frac{1}{T^{1\cdot3}}$ diagram for some aliphatic and cyclic sulphides.

FIG. 13. $\log P - \frac{1}{T^{1\cdot2}}$ diagram for water.

VOL. 5 1956

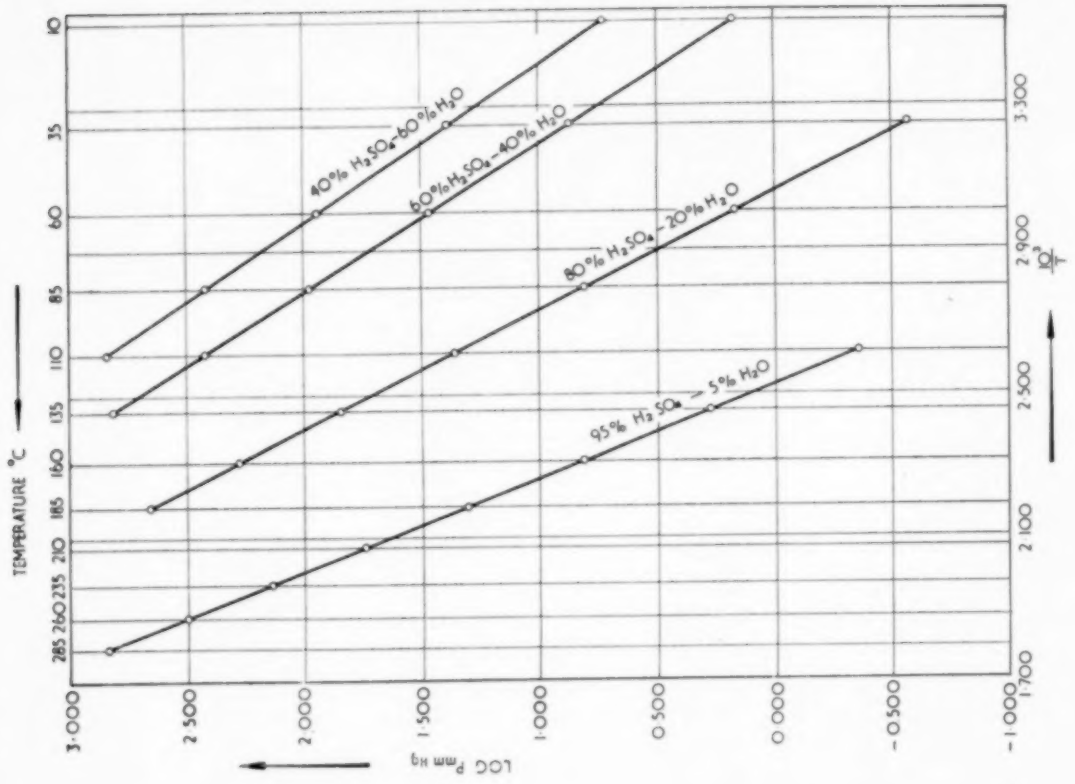

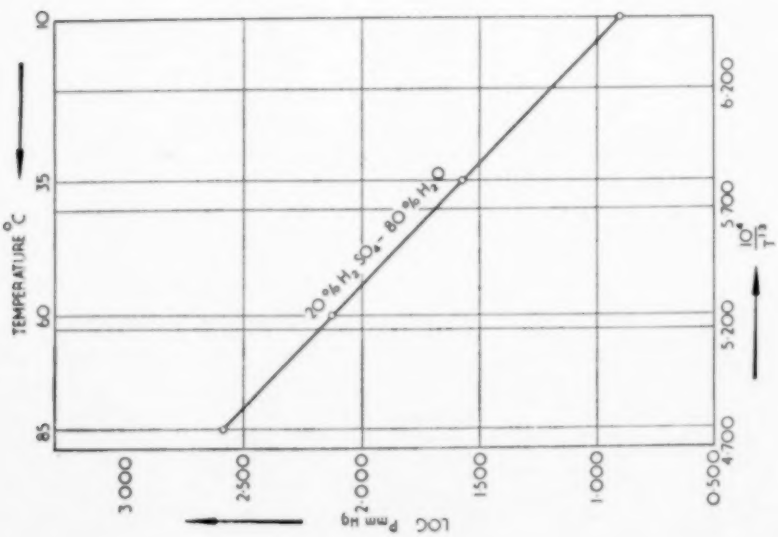

Fig. 14. $\log P - \frac{1}{T^{1\cdot3}}$ diagram for a mixture of 80 % H_2O and 20 % H_2SO_4.

Fig. 15. $\log P - \frac{1}{T}$ diagram for various concentrations of sulphuric acid in water.

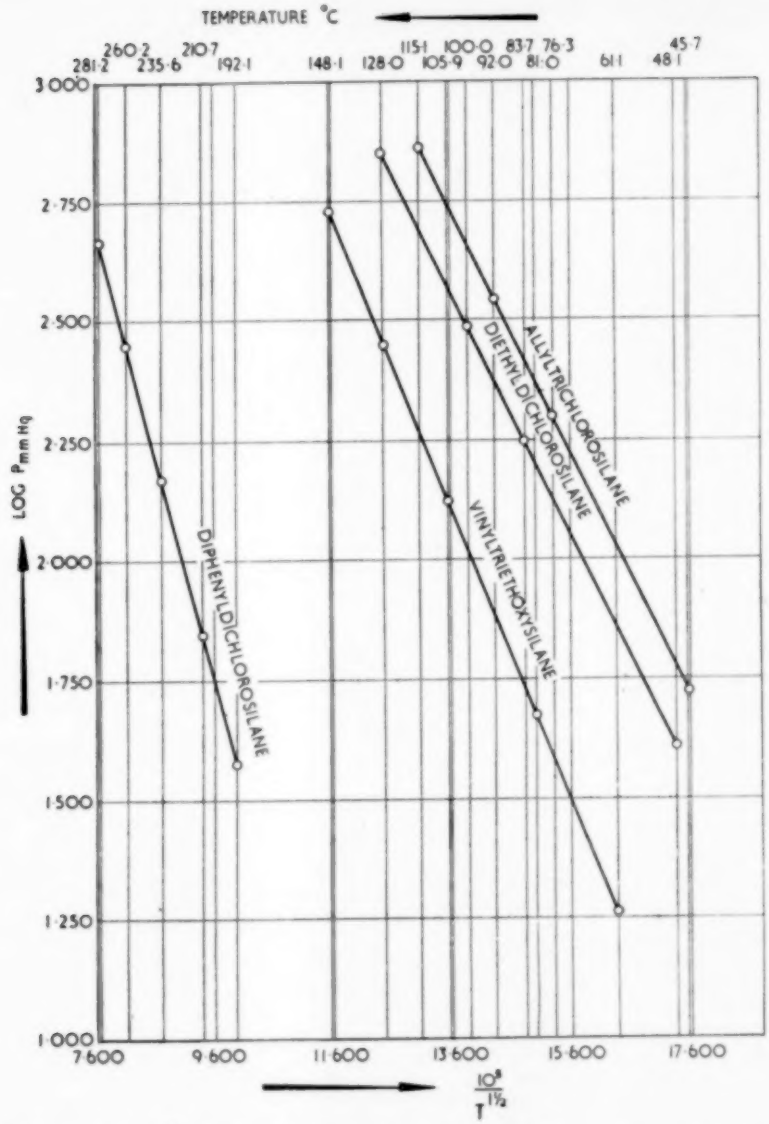

Fig. 16. $\log P - \frac{1}{T^{1\cdot5}}$ diagram for some intermediates in the preparation of silicones.

value of $x = 1{\cdot}2$ was chosen to construct the diagram $\log P = f\left(\frac{1}{T^{1\cdot2}}\right)$ for water, Fig. 13.

Comparison between predicted values of P for water at temperatures T are reported in Table 3. No deviation larger than 1·0 to 1·5% occurs over the whole temperature range.

According to Table 4 the values of x of water-sulphuric acid mixtures tend to decrease (from 1·3 to 1·0) with increasing sulphuric acid concentration (from 20% to 95% by weight). Plots of these various mixtures were constructed in diagrams representing $\log P = f\left(\frac{1}{T^{1\cdot3}}\right)$ and $\log P = f\left(\frac{1}{T^{1\cdot0}}\right)$ (see Figs. 14 and 15).

Good results are obtained when predicting the

VOL. 5 1956

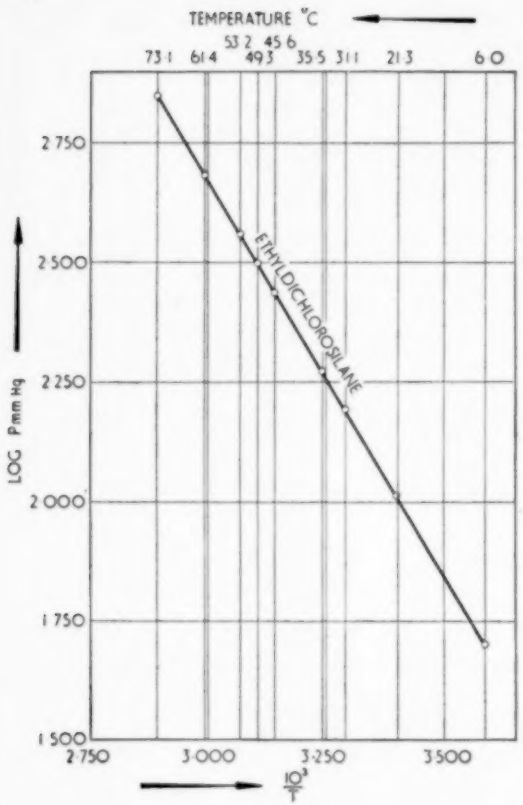

FIG. 17. $\log P - \frac{1}{T}$ diagram for ethyldichlorosilane.

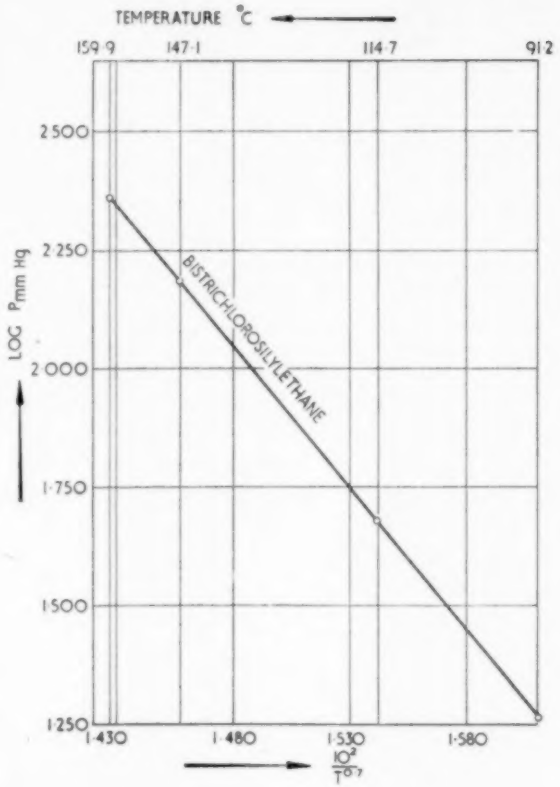

FIG. 18. $\log P - \frac{1}{T^{0.7}}$ diagram for bistrichloroethane.

values of P at various temperatures T from these diagrams, as can be seen from Table 4 : deviations generally are less than 1·5%. Data for water were taken from HODGMAN's Handbook [14] and for water-sulphuric acid mixtures from the I.C.T. [15].

The last group of substances is formed by intermediates in the preparation of silicones, *viz.*

Allyltrichlorosilane	$x = 1{\cdot}68$	Fig. 16
Ethyldichlorosilane	$x = 1{\cdot}06$	Fig. 17
Vinyltriethoxysilane	$x = 1{\cdot}42$	Fig. 16
Diethyldichlorosilane	$x = 1{\cdot}44$	Fig. 16
Diphenyldichlorosilane	$x = 1{\cdot}65$	Fig. 16
Bistrichlorosilylethane $Cl_3\,Si\,C_2\,H_4\,Si\,Cl_3$	$x = 0{\cdot}74$	Fig. 18

The value of x of four of these compounds a value of x of about 1·0, and a sixth one of 0·7. appeared to be about 1·5 ; a fifth compound had Corresponding plots of $\log P = f\left(\frac{1}{T^x}\right)$ were constructed, see Figs. 16, 17 and 18.

Data were taken from the literature [16]. As can be seen from Table 5 prediction of the values of P at various temperatures is possible without making errors exceeding about 1·5%.

From the above examples and considerations it can be concluded that graphical predictions of vapour pressures at some temperature T is possible to within 1·5%, even if the value of x in the graphical representation deviates some tenths from the exact value. It is interesting to examine at least one case in which the precise value of x has been calculated. The authors have done this and have chosen 1,1-dimethylcyclohexane. The

value of x had to be calculated in this case by means of the method of trial and error from three experimental measurements, *viz.* at 15·498°C, 67·558°C and 88·736°C. Data were taken from the literature [17]. The values of the three constants A, B and x from equation (2) appeared to be

$$A = 6{\cdot}23903$$
$$B = -10371{\cdot}7$$
$$x = 1{\cdot}3645$$

With the aid of these three constants, values of P at other temperatures were calculated and compared with the experimental data, see Table 6. From the table it appears that excellent agreement exists; no deviation larger than 0·2% occurs, and most deviations are within 0·02-0·05% or lower.

The authors have undertaken the study as a part of their extensive investigations on the correlation of physical constants and their dependence on chemical structure. Before, it was already mentioned that the authors prefer from all the formulae considered the formula (2)

$$\log P = \frac{A}{T^x} + B \qquad (2)$$

The reason of this preference is that analogous formulae can be used for the relation between other physical constants and the temperature. In this respect the formula

$$\log \nu = \frac{A}{T^x} + B \qquad (1)$$

was already mentioned. Formula (1) is an exact experimental relation between the kinematic viscosity and the temperature. Thus it is possible to compare different physical constants in an easy way. By applying these exponential formulae it is possible in cases where the exponents of the temperature are incidentally the same to derive simple relations between the physical constants in question. If *e.g.* in $\log \nu = \frac{A}{T^x} + B$ the exponent x is equal to the analogous exponent x in the formula $\log P = \frac{A}{T^x} + B$, a linear relationship exists between $\log P$ and $\log \nu$.

$$\log P = a \log \nu + b \qquad (14)$$

in which a and b are constants independent of the temperature.

The authors hope to continue their investigations in this direction.

Acknowledgements—The authors render their thanks to Mr. W. A. DAMMERS and Mr. F. SJENITZER for valuable comments in the preparation of this paper.

REFERENCES

[1] CORNELISSEN, J. and WATERMAN, H. I.; *Chem. Eng. Sci.* 1955 **4** 238.
[2] DALTON, J.; *Mem. Proc. Manchester Lit. & Phil. Soc.* 1801 **5** 550. Reference in THOMSON, G. W.; *Chem. Rev.* 1946 **38** 1.
[3] ANTOINE, C.; *Compt. rend.* 1888 **107** 681, 836, 1143.
[4] SCHMIDT, A.; *J. chim. phys.* 1917 **15** 97-153.
[5] CALINGAERT, G. and DAVIS, D. S.; *Industr. Eng. Chem.* 1925 **17** 1287-9.
[6] RANKINE, W. J. M.; *Edinburgh New Phil. J.* 1849 **94** 235. Reference in THOMSON, G. W.; *Chem. Rev.* 1946 **38** 1.
[7] KIRCHHOFF, G.; *Ann. Phys.* 1858 **104** 612.
[8] WIJS, J. C. DE; *Rec. trav. chim.* 1943 **62** 455.
[9] NERNST, W.; *Gött. Nachr.* 1906 **1**. Reference in THOMSON, G. W.; *Chem. Rev.* 1946 **38** 1.
[10] CHWOLSON, O. D. (Editor); *Traité de physique*, Vol. 3 1910 766-78, Paris.
[11] THOMSON, G. W.; *Chem. Rev.* 1946 **38** 1.
[12] HENGLEIN, F. A.; *Z. Phys. Chem.* 1921 **98** 1.
[13] Selected values of physical and thermodynamic properties of hydrocarbons and related compounds, American Petroleum Institute Research Project 44.
[14] HODGMAN, C. D.; *Handbook of Chemistry and Physics*, 30th edition, 1947, p. 1827-1831.
[15] International Critical Tables **3** 303.
[16] JENKINS, A. C. and CHAMBERS, G. F.; *Industr. Eng. Chem.* 1954 **46** 2367.
[17] FORZIATI, A. F., NORRIS, W. R., and ROSSINI, F. D.; *J. Res. Nat. Bur. Stand.* 1949 **43** 555.

VOL. 5 1956

Chemical Engineering Science, 1956, Vol. 5, pp. 161 to 167. Pergamon Press Ltd.

The partial coefficient of heat transfer in a drying fluidized bed

P. M. Heertjes and S. W. McKibbins*

Laboratory for Chemical Engineering, Delft Technical University, Delft.

(*Received* 18 *July*, 1955)

Abstract—The determination of the partial coefficient of heat transfer from air to a drying fluidized mass of silicagel is given. The data obtained can be correlated by means of the equation $h = 1{\cdot}31\,(R)^{0{\cdot}76}$.

A comparison of the external and internal heat exchange in a fluidized mass is presented.

Résumé—Les auteurs ont déterminé le coefficient de transfert de la chaleur cédée au cours du séchage par l'air à une masse de silicagel fluidisée ; ils ont exprimé leurs résultats à l'aide de l'équation : $h = 1{\cdot}31\,(R)^{0{\cdot}76}$, et comparé l'échange interne et externe dans une masse fluidisée.

VOL.
5
1956

It has been found earlier [1] that the drying of silicagel in a fluidized bed, in an adiabatic cylindrical apparatus with a sieve takes place in a comparatively small region. Moreover the temperature of the gel, with the exception of a small region near the sieve, and under certain circumstances, near the walls, is independent of the place in the apparatus. As in beds deeper than the region mentioned, this temperature by definition is equal to that of the air leaving the bed : the constant rate period of drying in principle offers an excellent means for determining the partial coefficient of heat transfer in the bed, because in that region the temperature of the gel is constant and easily to measure.

For the realization, however, the entrance effect (transport of heat through the sieves) has to be reduced to zero. This can be done in two ways ; by taking a very thin sieve with negligible resistance, or by eliminating the sieve altogether.

By construction of an apparatus in such a manner that the bed was entirely supported by the incoming air, the unequality of the parts of the apparatus caused such uneven velocity – and temperature distribution – that an easy evaluation was not possible. A report on the results of such an apparatus will be given later.

The method first mentioned was therefore chosen. Based on the facts found earlier, a very thin nylon gauze was used as a sieve. This material could be stretched tightly, and also had a negligible resistance, and therefore showed no sizeable entrance effect.

With such an apparatus the partial coefficient for heat transfer, h, was determined. It was also the intention to measure the partial coefficient of mass-transfer, k, with the view also of checking the well-known correlation : $h/k = \bar{\rho}\,\bar{c}_p\,(Le)^{1-n}$ (in which n to all probability $= \frac{1}{3}$), for which the system is very well suited. However, the measurement of the humidity with a Foxboro Dew-point recorder failed us, by lack of a sufficient accuracy in the lower humidity-regions. These measurements are being repeated with a different experimental way of determining the humidity, and will be presented in due time.

Apparatus and Procedure

The apparatus used and the procedure followed is substantially the same as described in the paper mentioned [1]. In the present research, however, an apparatus of a methacrylate plastic with a low coefficient of heat transfer was used, and moreover a vacuum existed between the walls of the fluidization chamber. For convenience sake a sketch of the fluidization chamber is given in Fig. 1. It is felt that this figure needs no further explanation.

* Present address : Wisconsin University, U.S.A.

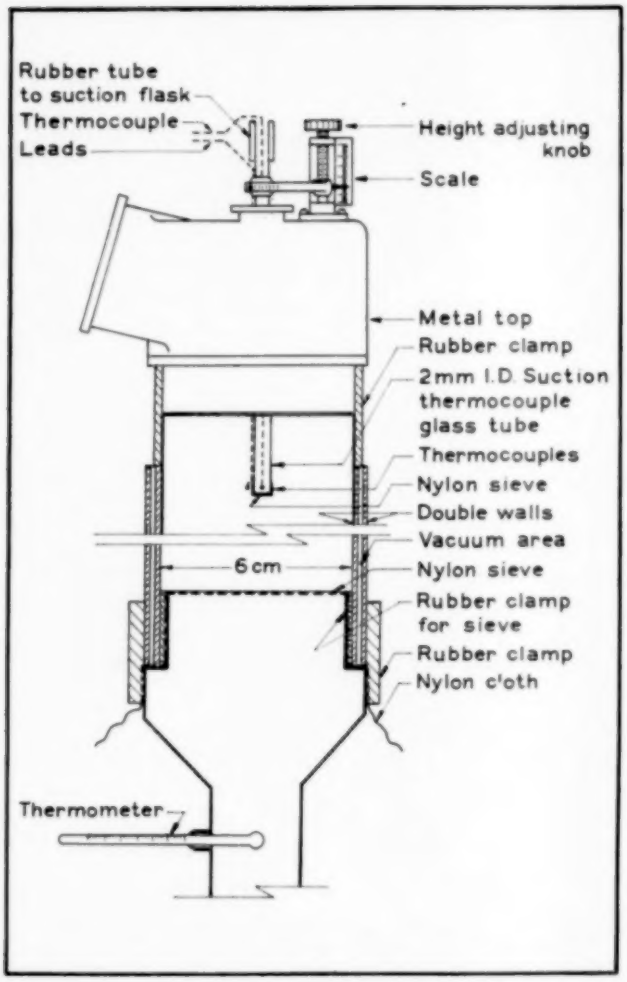

FIG. 1. The fluidization apparatus.

THEORY OF CALCULATION

From the experiments will result the temperature in the bed, t_g, and the temperature of the gel, t_s, as a function of the height, L, above the sieve. From these results the coefficient h, can be calculated in the following manner.

For an adiabatic apparatus in the constant rate period of drying the temperature of the gel is constant. Moreover, the surface temperature of the wall by the low thermal conductivity of the insulating system will be substantially equal to the gel temperatures, whereas the sieve has no resistance.

A heat balance in the bed between two horizontal planes at a distance dL therefore will give :

$$dq_s + dq_g = 0 \tag{1}$$

or

$$ha\,(t_g - t_s)\,dL + c_p\,GS\,dt_g = 0. \tag{2}$$

Assuming that all quantities are constant except the temperature, t_g, and the height, L, in view of the fact that t_s is constant, equation (2) can be integrated and gives between the limits L and O :

$$\ln \frac{(t_g - t_s)_0}{(t_g - t_s)_L} = \frac{ah}{c_p\,GS}\,L \tag{3}$$

A plot of $\ln \dfrac{(t_g - t_s)_0}{(t_g - t_s)_L}$ versus L should show a straight line, which passes through the origin and has a slope $s = \dfrac{ah}{c_p\,G\,S}$. From s the coefficient h can be calculated.

EXPERIMENTAL RESULTS

In the constant rate period of drying the results of each experiment can be presented graphically as in Fig. 2. If this figure is compared with Figs. 11 and 12 of the paper mentioned above, the differences caused by the entrance-effect are clearly demonstrated. With the aid of Fig. 2 $ln \dfrac{(t_g - t_s)_0}{(t_g - t_s)_L}$ can be calculated for any L. Some of the points found are plotted in Fig. 3. A straight line can indeed be drawn through the

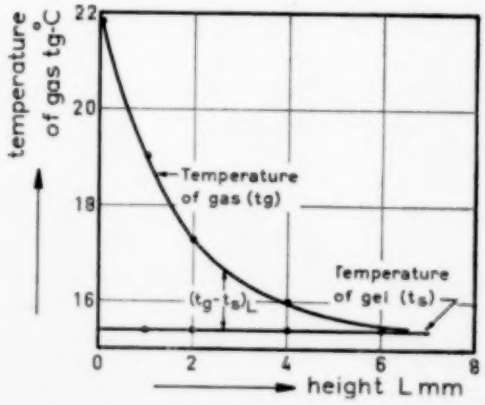

FIG. 2. The temperature of the air and the gel as a function of the height above the sieve.

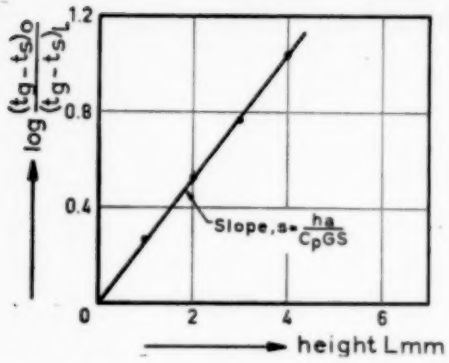

FIG. 3. $\log \frac{(t_g - t_s)_0}{(t_g - t_s)_L}$ as a function of the height above the sieve.

points, which passes the origin, as demanded by equation (3).

The slope enables the calculation of h provided that the surface area per unit height a can be found. For want of better information, it has been assumed that the porosity of the bed is the same at every point. This is not true, but information about the porosity as a function of the place in the bed and of experimental conditions so far is lacking. Moreover, beds of the type used are fairly homogeneous.

Taking the surface of the particles – which have been assumed apherical – as the surface of heat exchange,

$$a = \frac{6\,w}{\rho_s\, D_p\, L_{tot}} \qquad (4)$$

in which w = total weight and L_{tot} = total length of the fluidized bed.

In the experiments, the diameter of the particles (D_p, taken as the arithmetic mean) ranging from 0·36 to 1·1 mm, and the mass velocity of the air, G, ranging from 324 to 630 lbs./hr. ft^2, have been changed. The incoming air had a temperature of about 21°C and a dew-point of 13°F. Although up to 60°C the air temperature was found not to influence the results materially, this temperature was used because it allowed a reasonably slow rate of drying during which measurements could be more easily taken, and because it minimized the temperature difference between the bed and the outside air, and consequently reduced the heat losses through the walls of the reactor.

To ensure that the gel used in successive experiments was of constant water content, it was freshly humidified before each experiment by fluidizing it with air of constant maximal humidity until the gel and the air leaving reached a constant temperature.

The results of the experiments are given in Table 1. Heat balances showed differences of 5%, which prove that the departure of adiabatic conditions was not great.

Conclusions

Several methods were tried to correlate the data found. The fact that the Prandtl number was in all cases near unity, and that moreover its change was small, hampered the evaluation.

For the moment the best correlation found takes the form :

$$h = c\,(R)^m$$

A plot of $\log h$ versum $\log R$ as given in Fig. 4 demonstrates that the points can be connected with a straight line. From the method of the least squares the relationship was found to be :

$$h = 1{\cdot}31\,(R)^{0{\cdot}76} \qquad (5)$$

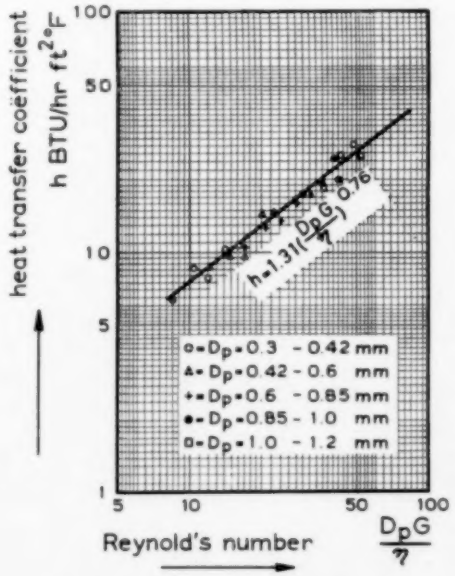

FIG. 4. $\log h$ as a function of $\log R$.

Table 1.

D_p-mm	G — $\frac{\text{lb.}}{\text{hr. ft.}^2}$	*Reynold's Number* $\frac{D_p G}{\eta}$	*Slope* s-1/ft.	$\frac{\bar{c}_p GS}{a}$	h-BTU/hr. ft.^{2} °F	h average
0·3–0·42	324	8·8	226	0·0278	6·3	
0·3–0·42	324	8·8	233	0·0278	6·5	6·4
0·3–0·42	324	8·8	236	0·0278	6·5	
0·3–0·42	324	8·8	230	0·0278	6·4	
0·3–0·42	391	10·6	242	0·0355	8·6	
0·3–0·42	391	10·6	250	0·0355	8·9	8·6
0·3–0·42	391	10·6	245	0·0355	8·7	
0·3–0·42	391	10·6	239	0·0355	8·5	
0·3–0·42	391	10·6	252	0·0355	8·9	
0·3–0·42	391	10·6	228	0·0355	8·1	
0·3–0·42	445	12·1	183	0·0410	7·5	
0·3–0·42	445	12·1	191	0·0410	7·85	
0·3–0·42	445	12·1	184	0·0410	7·5	7·9
0·3–0·42	445	12·1	214	0·0410	8·7	
0·3–0·42	445	12·1	224	0·0410	9·2	
0·3–0·42	526	14·3	231	0·0506	11·7	
0·3–0·42	526	14·3	188	0·0506	9·5	10·2
0·3–0·42	526	14·3	204	0·0506	10·3	
0·3–0·42	526	14·3	203	0·0506	10·3	
0·3–0·42	600	16·3	165	0·0575	9·5	
0·3–0·42	600	16·3	191	0·0575	11·0	10·6
0·3–0·42	600	16·3	193	0·0575	11·1	
0·42–0·6	324	12·45	219	0·0405	8·9	
0·42–0·6	324	12·45	199	0·0405	8·1	8·9
0·42–0·6	324	12·45	238	0·0405	9·7	
0·42–0·6	391	15·0	187	0·0493	9·3	
0·42–0·6	391	15·0	202	0·0493	10·0	9·9
0·42–0·6	391	15·0	212	0·0493	10·4	
0·42–0·6	445	17·1	181	0·0562	10·1	
0·42–0·6	445	17·1	172	0·0562	9·7	9·9
0·42–0·6	445	17·1	177	0·0562	9·9	
0·42–0·6	526	20·2	200	0·0700	14·0	
0·42–0·6	526	20·2	219	0·0700	15·3	14·6
0·42–0·6	526	20·2	210	0·0700	14·7	
0·42–0·6	526	20·2	206	0·0700	14·4	
0·42–0·6	600	23·0	179	0·0795	14·3	
0·42–0·6	600	23·0	190	0·0795	15·1	14·6
0·42–0·6	600	23·0	179	0·0795	14·3	

VOL. 5 1956

Table 1 (*continued*)

D_p–*mm*	G – $\frac{\text{lb.}}{\text{hr.ft.}^2}$	*Reynold's Number* $\frac{D_p G}{\eta}$	*Slope* s–1/ft.	$\frac{c_p GS}{a}$	h–BTU/hr. ft.^{2} °F	h average
0·6–0·85	324	17·6	202	0·0551	11·1	
0·6–0·85	324	17·6	193	0·0551	10·6	10·4
0·6–0·85	324	17·6	173	0·0551	9·6	
0·6–0·85	391	21·2	210	0·0666	14·0	
0·6–0·85	391	21·2	197	0·0666	13·1	12·9
0·6–0·85	391	21·2	175	0·0666	11·7	
0·6–0·85	445	24·1	179	0·0775	13·9	
0·6–0·85	445	24·1	169	0·0775	13·1	13·5
0·6–0·85	445	24·1	175	0·0775	13·6	
0·6–0·85	526	28·5	161	0·0958	15·4	
0·6–0·85	526	28·5	179	0·0958	17·1	16·0
0·6–0·85	526	28·5	172	0·0958	16·5	
0·6–0·85	526	28·5	156	0·0958	15·0	
0·6–0·85	600	32·5	154	0·109	16·8	17·4
0·6–0·85	600	32·5	165	0·109	18·0	
0·85–1·0	445	30·9	166	0·1035	17·2	17·4
0·85–1·0	445	30·9	169	0·1035	17·5	
0·85–1·0	526	36·5	158	0·122	19·3	19·5
0·85–1·0	526	36·5	161	0·122	19·6	
0·85–1·0	600	41·6	179	0·139	24·8	24·7
0·85–1·0	600	41·6	177	0·139	24·6	
0·85–1·0	630	43·7	137	0·146	20·0	20·0
0·85–1·0	630	43·7	136	0·146	19·9	
1·0–1·2	445	36·9	147	0·122	18·1	18·5
1·0–1·2	445	36·9	154	0·122	18·8	
1·0–1·2	526	43·6	175	0·146	25·6	
1·0–1·2	526	43·6	163	0·146	23·8	25·1
1·0–1·2	526	43·6	178	0·146	26·0	
1·0–1·2	600	49·8	175	0·166	29·1	28·5
1·0–1·2	600	49·8	167	0·166	27·8	
1·0–1·2	630	52·3	151	0·175	26·4	25·6
1·0–1·2	630	52·3	140	0·175	24·5	
1·0–1·2	630	52·3	149	0·175	26·1	

Table 2

G in lb./hr. ft.^{2}		300			500			700		
D_p in {ft. 10^{-3}}		1	2	3	1	2	3	1	2	3
h	WALTON *et al.*	3·7	5·5	6·8	9·3	13·2	16·2	16·5	23·4	28·7
	Present authors	5·6	9·6	13·0	8·3	14·1	19·2	10·8	18·2	24·8

The results obtained in these experiments differ from those of SMITH *et al.* [2]. Correlation of their data in the manner described gives rather scattering points, with the exponent m close to 0·76, but with a much lower constant c. The difference can be explained by the fact that SMITH *et al.* for the measurement of the gas temperature in the rather dense bed, used a bare thermocouple, which, owing to the spasmodic bombardment of the gel particles, will show a greater tendency to vary, whereas invariably a lower temperature will be found because the gel temperature is lower than the air temperature.

A far better agreement exists with the values obtained by WALTON *et al.* [3],whose results came to our knowledge after our work had been finished. Table 2 will indicate that the order of magnitude of h is in both cases the same. The values have been calculated by means of the correlations given.

The experiments of WALTON *et al.* were carried out at a temperature of 100°C.

If D_p is expressed in feet, their correlation takes the form,

$$h = 0{\cdot}0076\,(G)^{1{\cdot}7}\,(D_p)^{0{\cdot}5} \qquad (6)$$

This is a different form of correlation as found by the present authors, who have tried to present their results in the form of equation (6). The data show a much greater tendency to scatter as compared with eq. (5). An approximate correlation with G and D_p separated was found to be

$$h = 7{\cdot}4\,(G)^{0{\cdot}76}\,(D_p)^{0{\cdot}67},$$

which indicates that D_p and G both affect the heat transfer coefficient to approximately the same extent.

For the present author's experiments therefore equation (5) gives the best correlation. More experiments with greater variation in D_p and G (if possible) will be needed to obtain the correct correlation. Moreover, although the ranges in D_p and G involved in both researches are the same, small differences in the type of fluidization can have a rather large influence on the correlation given. Also, in WALTON *et al.* experiments there is still a small incertitude with regard to the temperature of the solid substance.

It is interesting to compare the partial coefficient of heat transfer with gas alone, h_v, and in a fluidized bed, h_{fe}, to the walls of the chamber with the same coefficient, h_{fi}, for internal heat transport, for the same mass rate of flow. Moreover, the product, p, of h with the heat exhanging surface is interesting. The figures of Table 3 have been collected for a tube cf 1 ft. length, a diameter of 0·1 ft. and 0·3 ft. respectively, with particles of 300 μ and a mean porosity of the bed of 60%. The coefficient h_v has been calculated with the

Table 3

	h_v		h_{fe}		h_{fi}
	0·4		52		5·2
p for a tube of 0·1 ft. diameter :	1·3		163		9,960
ratio	1	:	125	:	7,800
p for a tube of 0·3 ft. diameter :	3·8		490		89,640
ratio :	1	:	125	:	24,000

VOL. 5 1956

Dittus-Boelter equation, h_{fe}, with the correlation of VAN HEERDEN *et al.* [4].

The great heat-equalizing power of the fluid bed is clearly demonstrated by these figures. The same influences of the fluidized bed on the heat transport to the walls seem to appear in the internal heat transport. The disrupture of the viscous film of air seems to be however not so strong as at the walls, moreover the contact between the particles is of a shorter time and is less frequent.

NOMENCLATURE

a	= surface per unit of length of fluidized bed	(ft.)
c	= constant	(BTU/ft.^{2}hr.°F)
c_p	= specific heat at constant pressure	(BTU/lb. °F)
D_p	= diameter of particle	(ft.)
G	= mass velocity	(lb./ft.^{2} hr)
h	= partial coefficient of heat transfer	(BTU/ft.^{2} hr °F)
L	= length of fluidized bed	(ft.)
Le	= Lewis number	no dimension
m	= constant	no dimension
n	= constant	no dimension
p	= product of h with the surface of heat exchange	(BTU/hr. °F)
q	= amount of heat	(BTU/hr.)
R	= Reynolds number	no dimension
s	= slope of line	(l/ft.)
S	= cross-section of fluidization-chamber	(ft.^{2})
t	= temperature	(°F)
w	= weight of silicagel in the bed	(lb.)
ρ	= density	(lb./ft.^{3})

Subscripts

fe	= for the tube with the fluidized mass to the walls
fi	= for the gas to the fluidized mass
g	= of the gas
L	= at height L
o	= at height zero
s	= of the silicagel
tot	= at total height of the bed
v	= for the tube without fluidized mass to the walls

REFERENCES

[1] HEERTJES, P. M., de BOER, H. G. J., and de HAAS VAN DORSSER, A. H.; *Chem. Eng. Sci.* 1953 **2** 97.

[2] KETTENRING, K. N., MANDERSFIELD, E. L., and SMITH, J. M.; *Chem. Eng. Prog.* 1950 **46** 139.

[3] WALTON, J. S., OLSEN, R. L., and LEVENSPIEL, O.; *Ind. Eng. Chem.* 1952 **44** 1474.

[4] VAN HEERDEN, C., NOBEL, P., and VAN KREVELEN, D. W.; *Chem. Eng. Sci.* 1951 **1** (vol. 2) 51.

Chemical Engineering Science, 1956, Vol. 5, pp. 168 to 177. Pergamon Press Ltd.

The calibration of disc-type laboratory gas-absorption columns

R. F. Taylor and F. Roberts

Chemical Engineering Division, A.E.R.E., Harwell, Didcot, Berks.

(*Received* 19 *August* 1955)

Abstract—The disc column [17, 12] has been examined from the calibration standpoint, using two systems : carbon dioxide into water, and dilute ammonia gas into water.

The plots of film coefficient versus liquid rate show a distinct change of slope, not previously reported ; this break coincides with the establishment of ripple formation on the rims of the discs.

The film coefficients were consistently below those of Stephens and Morris, but differences in calibration between different disc columns are not uncommon. Some workers have found it difficult to wet the discs successfully. However, in this work wetting was successfully achieved by systematically roughening pyrophyllite discs, and keeping them wet between runs.

Résumé—Les auteurs ont étudié l'étalonnage d'une colonne à disques [17, 12] au moyen des deux systèmes : CO_2 dans l'eau et ammoniac dilué dans l'eau.

Les courbes du coefficient laminaire d'échange en fonction de la vitesse du liquide montrent une variation nette de la pente qui n'a pas été signalée ; cette cassure coïncide avec la formation de rides sur le bord des diquses.

Les coefficients sont sensiblement inférieurs à ceux de Stephens et Morris, mais il y a souvent des différences dans le calibrage des disques de colonnes que certains auteurs ont éprouvé des difficultés à mouiller correctement.

Un mouillage parfait a été obtenu dans le cas des disques de pyrophyllite, grâce à un dépolissage systematiqué et la conservation à l'état mouillé entre les expériences.

VOL.
5
1956

Introduction

The disc column was introduced by Stephens and Morris [17, 12] as a development of the wetted-wall column " in which the film of liquid was interrupted at short intervals during its descent, thus simulating the conditions of flow over a packing." Details of the apparatus, methods of calibration, and an example of its use in problems of absorption in the presence of chemical reaction, are given in these references.

It has been used on a number of different chemical systems [17, 13, 14, 11, 1], and Warner [18] examined the gas flow characteristics of the column. Danckwerts [3] and Hoftyzer [9] commented on differences between the hydrodynamics of packed towers and those of the disc column, and drew attention to limitations of the latter as a model of the former.

Stephens and Morris stressed that a column should be calibrated on a known system because the absorption coefficients obtained on different columns might vary by $\pm 10\%$. The absorption of pure carbon dioxide into water was suggested as a suitable system for establishing the liquid film characteristics, and absorption of dilute ammonia gas into water for the gas film characteristics. During such calibration work the authors have found discrepancies between the results obtained and those quoted in the literature.

Experimental

In general the apparatus used and the procedures adopted closely followed those of Stephens and Morris [17], and their paper henceforth is referred to as " S. and M."

Apparatus—The various types of disc were threaded and cemented on stainless steel wire or Fiberglas thread which was held in tension inside the precision-bore glass tube. The precautions mentioned by S. and M. were embodied in the apparatus. The general arrangement, and other relevant details, are shown in Fig. 1. Dimensions are listed in Table 1.

Calming sections of 5 and 10 in. length were both

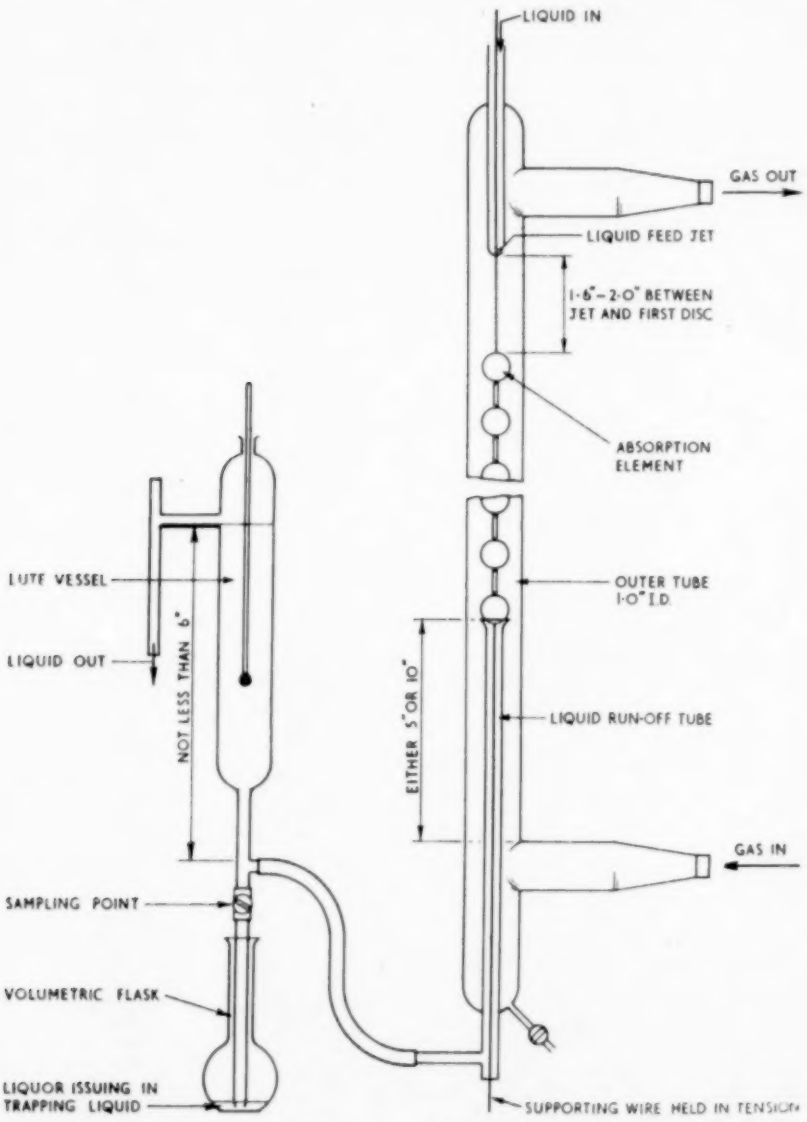

FIG. 1. Arrangement of absorption column.

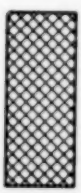

FIG. 1 (a). Roughened pyrophyllite disc. Both faces and rim scored by file. 20 cuts per inch in each direction. Approximately 1/50 in. to 1/100 in. deep. Knife needle file – Grade 2.

Table 1.

Type of disc	*Doulton*	*Smooth Pyrophyllite*	*Rough pyrophyllite*	
Number of discs	61	60	60	50
Disc diameter – ins.	0·572	0·574	0·574	0·574
Disc thickness – ins.	0·193	0·175	0·175	0·175
Tube diameter – ins.	0·99	0·99	0·99	0·99
Mean perimeter for liquid flow – ft.	0·123	0·121	0·121	0·121
Equivalent diameter for gas flow – ft.	0·049	0·050	0·050	0·050
Free space (dry)	89%	90%	90%	90%
Absorption surface – ft^2	0·364	0·348	0·348	0·290

VOL. 5 1956

tested, but the coefficients obtained were essentially the same. Liquid temperatures were measured with calibrated thermometers, and checks were made on gas temperatures. The air and gas supplies were fed through calibrated rotameters, and in the case of the ammonia/air feed the combined stream was well mixed in a 25-litre vessel before entering the column.

Procedure—Distilled water was used as the absorbing liquor for both systems, and in the respective cases the feed was shown to be free of carbon dioxide and ammonia. Each run lasted 45 min, with three samples taken at 5 min intervals towards the end, in order to ascertain that equilibrium conditions had been reached.

In the carbon dioxide work, the gas was 99·2-99·8% pure. The liquid film coefficients obtained were corrected to a temperature of 20°C, using the relationship derived by Sherwood and Holloway [16].

In the ammonia absorption work the gas/air mixtures used contained 3-5% by volume NH_3. Analyses for the ammonia content were made on the gas and liquid streams entering and leaving the column. In no case did the error on the material balance exceed 6%. The temperature of the runs lay in the range 17-21°C. The gas film coefficient k_G was obtained following the method adopted by S. and M. The general equation [16] :

$$\frac{k_L}{D} = \alpha \left(\frac{4\Gamma}{\mu}\right)^n \left(\frac{\mu}{\rho D}\right)^{0.5} \ldots \text{ft}^{-1} \qquad (1)$$

was used to evaluate k_L at 20°C. The appropriate values for α and n were obtained from equation (3) or (4), according to the value of the wetting rate Γ (see below). Further points of interest in procedure are dealt with in the Appendix.

Results

The results of the present calibration work, shown in Tables 2, 3 and 4, and plotted in Figs. 2, 3 and 4, are somewhat different from those of S. and M. In the plot of liquid film coefficient versus wetting rate for carbon dioxide absorption (Fig. 2) the curve is lower than that of S. and M. and has a distinct change of slope. Both sets of results fit the general equation 1, viz.:

S. and M. giving

$$\frac{k_L}{D} = 21{\cdot}0 \left(\frac{4\Gamma}{\mu}\right)^{0.7} \left(\frac{\mu}{\rho D}\right)^{0.5} \ldots \text{ft}^{-1} \qquad (2)$$

whereas the present results give for $\Gamma < 155$ lb./-hr ft :

$$\frac{k_L}{D} = 58{\cdot}0 \left(\frac{4\Gamma}{\mu}\right)^{0.4} \left(\frac{\mu}{\rho D}\right)^{0.5} \ldots \text{ft}^{-1} \qquad (3)$$

and for $\Gamma > 155$ lb./hr. ft :

$$\frac{k_L}{D} = 1{\cdot}94 \left(\frac{4\Gamma}{\mu}\right)^{1.0} \left(\frac{\mu}{\rho D}\right)^{0.5} \ldots \text{ft}^{-1} \qquad (4)$$

Results of the calibration with ammonia/air mixtures into water are shown graphically in Figs. 3 and 4. In the plot of k_G versus relative velocity, the curve lies below and parallel to that of S. and M., both curves showing a similar break at a relative velocity of 3·6 ft/sec. The relative

Table 2. Absorption of CO_2 in water.

Run No.	Atmos. pressure Mm. Hg	Liquid rate lb/hr ft l'	Water temp. °C		CO_2 conc. out lb/cu. ft. $\times 10^{-2}$	CO_2 absorbed lb/hr $\times 10^{-2}$	Log mean driving force lb/cu. ft. $\times 10^{-2}$	Absorption coefficient lb/hr ft² lb/ft³	
			in	out				Observed	Corrected to 20°C
			61 Doulton Discs						
1	748	465	21·6	21·6	5·92	5·45	6·37	2·38	2·29
2	752	156	20·1	20·0	6·56	2·02	6·61	0·840	0·84
3	759	66·6	20·8	20·5	8·34	1·10	4·93	0·612	0·61
4	755	103	20·1	20·0	7·52	1·53	5·88	0·716	0·72
5	755	292	21·1	20·9	6·23	3·60	6·50	1·53	1·49
6	751	213	20·8	20·8	6·48	2·72	6·32	1·19	1·16
7	746	115	19·6	19·7	7·29	1·66	6·05	0·753	0·76
8	747	312	20·3	20·3	6·24	3·85	6·55	1·62	1·61
9	742	275	19·5	19·5	6·60	3·60	6·59	1·50	1·52
10	742	64·5	20·0	19·6	8·66	1·11	4·74	0·643	0·65
11	741	166	20·7	20·6	6·54	2·15	6·19	0·955	0·94
12	752	384	18·5	18·6	6·79	5·19	6·96	2·05	2·13
			60 Smooth Pyrophyllite Discs						
13	755	82	21·0	20·9	8·66	1·38	4·45	0·890	0·88
14	757	213	20·0	20·3	6·45	2·67	6·65	1·16	1·16
15	762	192	17·9	18·2	6·79	2·54	7·07	1·03	1·08
16	762	337	19·9	19·8	6·89	4·62	6·66	2·00	2·00
17	762	48	20·3	19·7	9·53	0·89	4·04	0·633	0·63
18	761	358	17·7	18·1	8·15	5·68	6·30	2·59	2·72
19	761	186	18·7	19·0	6·97	2·52	6·90	1·05	1·08
			60 Roughened Pyrophyllite Discs						
20	743	140	20·5	20·7	6·72	1·84	6·09	0·869	0·86
21	750	53	19·3	19·0	9·23	0·96	4·59	0·602	0·62
22	748	256	20·0	20·3	6·75	3·22	6·36	1·46	1·46
23	749	328	19·6	19·8	6·88	4·38	6·44	1·96	1·96
24	749	287	19·7	19·9	7·10	3·96	6·20	1·84	1·84
25	750	216	19·7	19·9	6·93	2·90	6·34	1·31	1·32
26	749	175	20·0	20·1	6·78	2·31	6·31	1·05	1·05
27	744	112	18·7	18·9	7·70	1·69	6·03	0·805	0·83
28	740	85	19·8	19·5	8·04	1·32	5·32	0·712	0·72
29	740	47	20·0	19·7	9·14	0·83	4·08	0·584	0·59
30	750	67	16·0	16·1	9·60	1·25	5·61	0·640	0·70
31	750	99	17·3	17·3	8·35	1·61	6·20	0·746	0·79
32	750	145	17·4	17·4	7·40	2·10	6·86	0·880	0·93
33	750	198	17·7	17·8	7·00	2·69	7·08	1·09	1·15
34	737	240	17·8	18·3	7·09	3·32	7·80	1·19	1·24
35	736	136	16·7	17·0	7·81	2·05	6·54	0·899	0·96
			50 Roughened Pyrophyllite Discs						
36	744	173	19·1	19·4	6·28	2·11	6·93	1·05	1·08
37	744	372	19·1	19·5	6·27	4·54	6·93	2·26	2·29
38	745	64	19·8	20·2	8·56	1·06	4·80	0·759	0·76

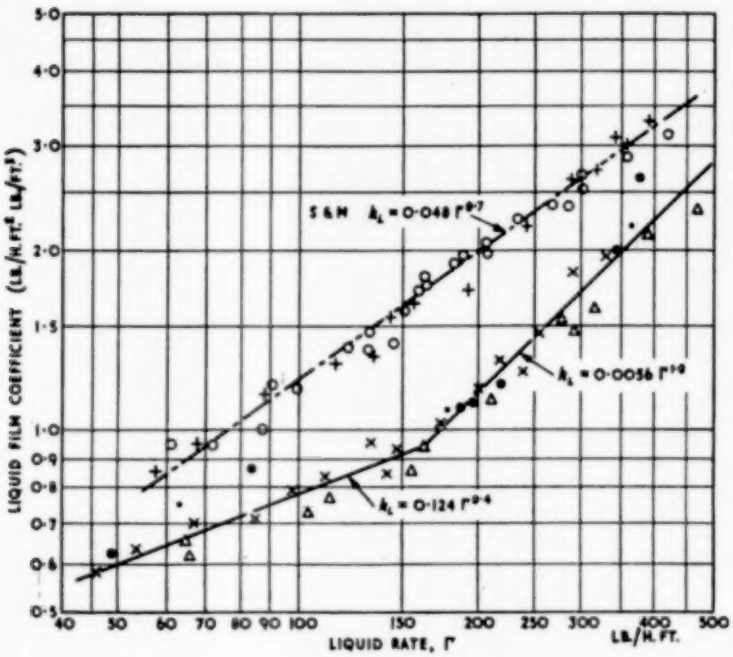

Fig. 2. Liquid film coefficients for absorption of carbon dioxide in water. Values corrected to a liquid temperature 20°C. Stephens and Morris: ○ – 40 disc column; + – 24 disc column. Taylor and Roberts: △ – 61 Doulton discs; ● – 60 smooth pyrophyllite discs; X – 60 roughened pyrophyllite discs; • – 50 roughened pyrophyllite discs.

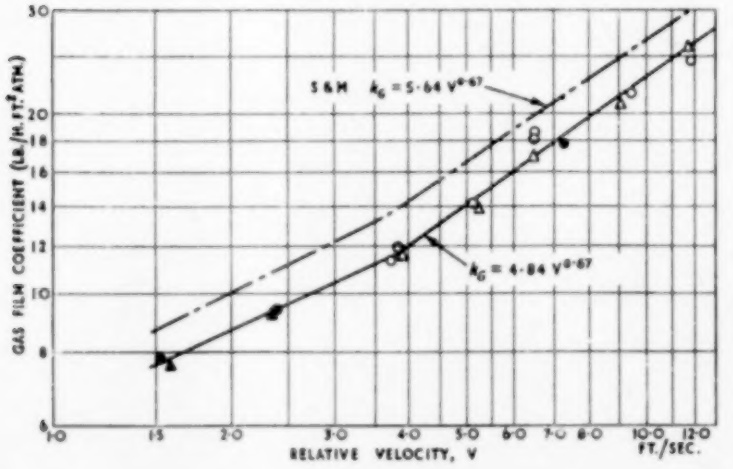

Fig. 3. Absorption of ammonia in water: effect of gas velocity on gas-film coefficient. △ – 61 Doulton discs – counter-current flow; ▲ – 61 Doulton discs – co-current flow; ○ – 60 rough pyrophyllite discs – counter-current flow; ● – 60 rough pyrophyllite discs – co-current flow. Constant liquid rate: (Γ = 274 lb/hr ft). Linear velocity of liquid = 1·14 ft/sec.

VOL. 5 1956

Table 3. *Absorption of ammonia in water. Variable gas velocity.*

Run No.	*Relative velocity ft/sec*	NH_3 *in exit liquid lb/cu. ft*	*Log mean driving force atm.*	*Overall coefficient lb/hr ft² atm*	*Gas film coefficient lb/hr ft² atm*	*Material balance %*
			61 Doulton Discs			
			Counter-current flow			
1	9·06	0·342	0·0266	18·8	20·6	102
2	11·72	0·414	0·0266	22·7	25·4	101
3	6·51	0·222	0·0219	15·6	16·8	96
4	3·85	0·127	0·0176	11·1	11·7	95
5	5·21	0·205	0·0228	13·0	13·9	105
			Co-current flow			
6	1·57	0·106	0·0228	7·28	7·54	96
7	2·33	0·139	0·0243	8·71	9·08	95
			60 Roughened Pyrophyllite Discs			
			Counter-current flow			
8	3·79	0·124	0·0183	10·4	11·4	104
9	5·14	0·172	0·0209	12·5	14·0	97
10	6·49	0·222	0·0210	15·9	18·5	95
11	9·44	0·338	0·0276	18·4	21·7	98
12	11·94	0·419	0·0322	20·2	24·7	106
13	3·78	0·133	0·0191	10·8	11·9	105
14	6·50	0·222	0·0214	15·7	18·1	97
			Co-current flow			
15	2·40	0·135	0·0238	8·70	9·39	99
16	1·54	0·105	0·0219	7·29	7·75	96
17	7·16	0·295	0·0291	15·5	17·8	101

Constant liquid rate = 274 lb/hr ft

velocity is calculated from the linear velocity of the gas and that of the liquid surface as derived by Cooper *et al.* [2]. Over the range of relative velocities v, 3·6-13 ft/sec, the equations of the two curves are :

S. and M. :

$$k_G = 5{\cdot}64\, v^{0{\cdot}67}, \text{ for } \Gamma = 236 \text{ lb/hr ft} \qquad (5)$$

Taylor and Roberts :

$$k_G = 4{\cdot}84\, v^{0{\cdot}67}, \text{ for } \Gamma = 274 \text{ lb/hr ft} \qquad (6)$$

When allowance is made for the difference in liquid rates the latter curve gives values of k_G 83% of those of S. and M. Warner [18] studied the gas-flow characteristics of the disc column in some detail, and found that changes in the gas flow behaviour took place in conditions given approximately by

$$v_G\, \rho^{0{\cdot}41}\, \Gamma^{0{\cdot}22} = 4 \qquad (7)$$

and

$$v_G\, \rho^{0{\cdot}41}\, \Gamma^{0{\cdot}22} = 12 \qquad (8)$$

These equations do not appear to take into account the *relative* velocity of the gas and liquid phases, but the break point indicated by equation (7) does approximate to the value obtained by S. and M. and the authors for *counter flow* conditions.

The effects of varying the liquid rate on ammonia absorption are shown in Fig. 4. The results are below those of S. and M. and show a break point not indicated by those authors. The equations of the curves are :

S. and M.

$$k_G = 11{\cdot}1\, \Gamma^{0{\cdot}13} \text{ lb/hr ft}^2 \text{ atm} \qquad (9)$$

T. and R. for $\Gamma < 155$ lb/hr ft :

$$k_G = 18{\cdot}5 \text{ lb/hr ft}^2 \text{ atm (slope 0)} \qquad (10)$$

Table 4. Absorption of ammonia in water. Variable liquor rate.

Run No.	*Liquid rate lb/hr ft*	*Relative velocity ft/sec*	NH_3 *in exit liquor lb/cu. ft*	*Log mean driving force atm.*	*Overall coefficient lb/hr ft² atm.*	*Gas film coefficient lb/hr ft² atm*		*Material balance %*
						Observed	*Corrected to V = 8·4 ft/sec*	
			61 Doulton Discs – *Counter current*					
1	168	8·8	0·519	0·0292	15·1	18·8	18·3	95
2	74	8·5	0·988	0·0284	13·0	17·2	17·2	102
			60 Rough Pyrophyllite Discs *Counter current*					
3	150	9·06	0·533	0·0299	14·9	18·9	18·0	100
4	64	8·73	1·06	0·0259	14·5	19·8	19·1	97
5	394	9·75	0·241	0·0238	22·3	25·6	23·2	101
6	326	9·58	0·292	0·0248	21·4	25·1	22·9	95
7	206	9·24	0·428	0·0277	17·6	21·8	20·4	96
8	101	8·90	0·737	0·0282	14·6	19·2	18·5	96
9	181	9·20	0·466	0·0272	17·1	21·8	20·3	97
10	233	9·31	0·383	0·0268	18·5	22·6	20·9	96
11	274	9·44	0·338	0·0276	18·4	21·7	20·3	98
				Co-current				
12	274	7·16	0·295	0·0291	15·5	17·8	20·1	101

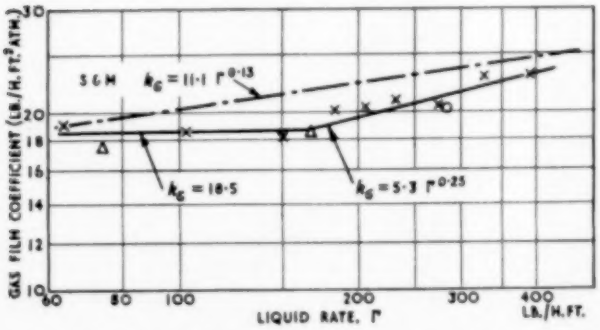

Fig. 4. Absorption of ammonia in water. Effect of liquid rate on gas-film coefficient. X – 60 rough pyrophyllite discs; O – 60 rough pyrophyllite discs – co-current flow; Δ – 61 Doulton discs. All values corrected to a relative velocity of 8·4 ft/sec.

for $\Gamma > 155$ lb/hr ft :

$$k_G = 5{\cdot}3\ \Gamma^{0.25}\ \text{lb/hr ft}^2\ \text{atm} \qquad (11)$$

Liquid Flow Behaviour

The plots of film coefficients versus liquid rate, for the various types of disc and the two chemical systems, show that the break point occurs at approximately the same liquid rate ($\Gamma = 155$ lb/hr ft). The columns of discs were examined visually at various liquid flow rates. The flow pattern on the *faces* of the discs appeared to be complicated, and no critical flow rates were detected. Examination of the flow round the *rim* of the discs, however, revealed a distinct change in flow pattern over a relatively small change in liquor rate. This change is shown in the photographs (Fig. 5). Immediately below the critical rate of $\Gamma = 155$, only transient ripple formation appears, and above it the ripple formations become permanent. (The *transient* nature of the ripples in Fig. 5 (b) is not, of course, evident from a photograph).

The flow rate at which ripples first become permanently established was measured for various types and sizes of disc, and the results given in Table 5 show that discs with the same dimensions have similar critical flow rates. A chain of discs of larger radius but similar thickness (type 4) had a different critical value in terms of the overall

VOL. 5 1956

OL.
5
956

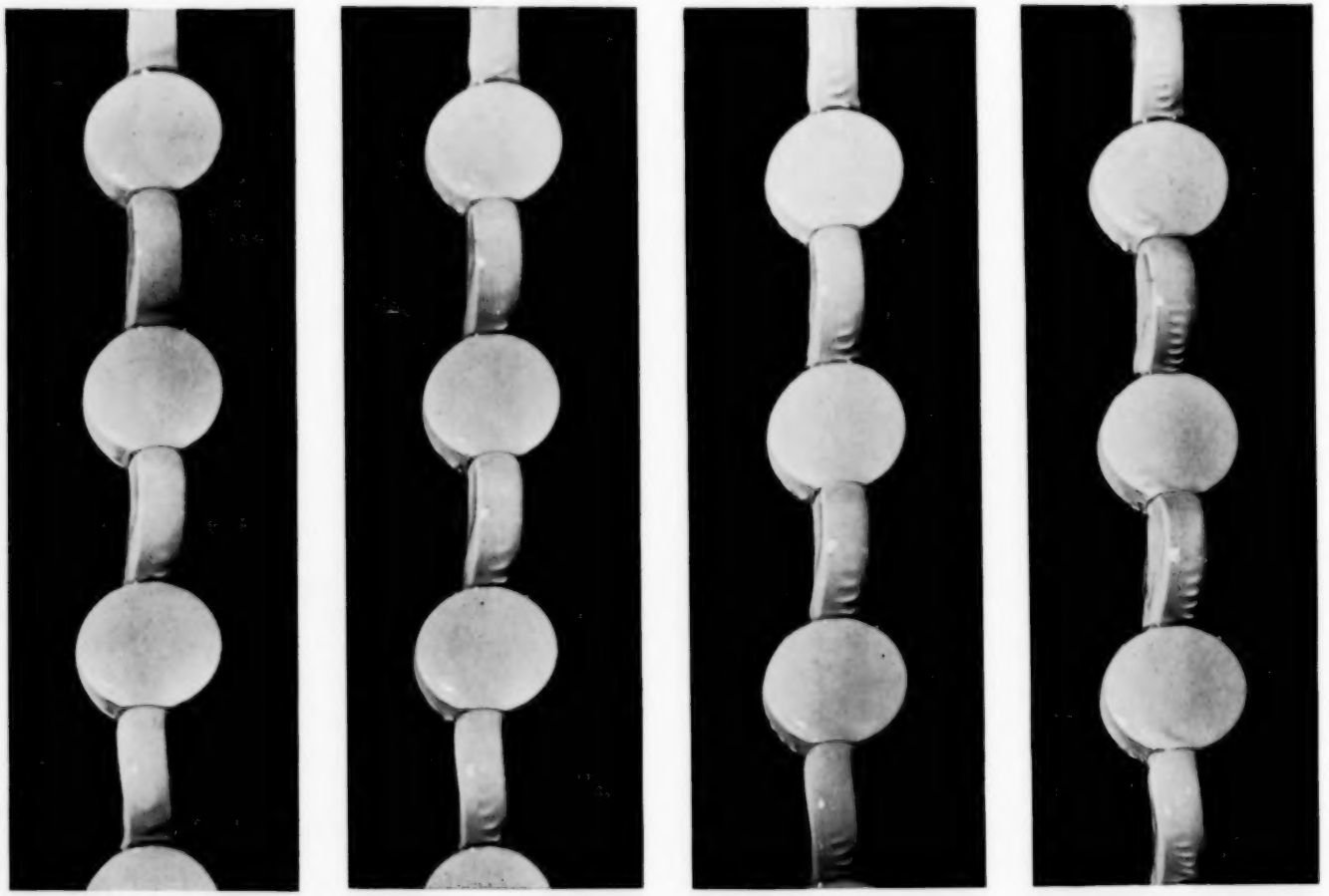

(*a*) $\Gamma = 99$ lb./hr.ft. (*b*) $\Gamma = 145$ lb./hr.ft. (*c*) $\Gamma = 165$ lb./hr.ft. (*d*) $\Gamma = 293$ lb./hr.ft.

FIG. 5. Formation of ripples on discs.

VOL.
5
1956

Table 5. Effect of disc dimensions on critical flow rate.

No.	*Type of disc*	*Thickness in.*	*Diameter in.*	*Critical flow lb/hr*	*Overall Γ lb/hr ft*	$\frac{\text{Critical flow}}{4 \times \text{thickness}} \propto$ "(local Γ at junctions)"
1	Doulton smooth ceramic	0·193	0·572	18·5	151	288
2	Rough sandstone (D. R. Morris)	0·207	0·597	20·3	154	295
3	Pyrophyllite roughened	0·175	0·574	18·0	150	308
4	Calcium fluoride, large diameter	0·252	1·054	25·2	134	300
5	Pyrophyllite, thick, smooth	0·407	0·610	18·1	97	133

wetting rate. Rippling begins at the disc junctions, where the perimeter is a minimum. It is therefore possible that the *local* wetting rate, based on this perimeter, might provide a better criterion for correlating critical flow rates; a value of four times the disc thickness may reasonably be used for the perimeter. With a very thick disc (type 5) the bulk of the liquid appeared to flow down the central portion of the rim, and this may account for the fact that the critical flow rate was similar to that for narrow discs of similar radius.

This type of ripple formation arises at flow rates much higher than those ($Re = 25$) mentioned by Grimley [7] and by D. R. Morris [11]. In view of the irregular irrigation of discs it is possible that local Reynolds numbers as high as 1,000-1,200 are reached in disc column experiments, and transition to turbulent flow takes place [4, 6]. It is thought that spheres should give a more regular distribution than discs, but this requires experimental proof.

Conclusions

The film coefficients obtained are self-consistent but below those published by S. and M., who did, however, recognize that differences between different disc-columns occurred. Other workers using the carbon dioxide system in disc columns have obtained varying results [5], and close control over techniques is essential if reliable data are to be obtained.

In the curves for film coefficient versus liquid rate a distinct change of slope has been found. This break has been correlated with the establishment of ripple formations on the rim of the discs, and for water flowing over the usual size of disc takes place at an overall wetting rate of about 155 lb/hr ft.

The wetting of conventional discs is not good, whereas that of pyrophyllite discs roughened by file, and soaked between runs, is excellent (details given in appendix). The irrigation of fully wetted discs are still complex, however, and tends to vary with different sizes of discs; the irrigation of spheres should be more regular.

Acknowledgements—The work described in this paper was carried out at A.E.R.E., Harwell, and thanks are due to the Director for permission to publish. The authors wish to express their thanks for helpful advice to Mr. G. A. Morris of I.C.I. Widnes, to members of the I.C.I. Billingham Division staff, and to Dr. D. R. Morris (late of King's College, London, and now at A.E.R.E.). Thanks are also due to Mr. R. A. Smith, Billingham, for the pyrophyllite discs.

Appendix

Factors Influencing Accuracy of Results

(a) *Liquor Sampling*—To ensure against loss of gas from samples of the outgoing liquor stream, they were taken from a well-flushed point six inches below the liquid surface. The samples issued below the surface of a substantial excess of trapping solution in a volumetric flask.

(b) *Methods of Analysis*—The ammonia liquor was trapped

in standard hydrochloric acid and the excess back titrated.

Three methods of analysis for carbon dioxide in water were examined. They were checked on saturated carbon dioxide solutions, and also on solutions of standard sodium carbonate which had been treated with the stoichiometric amount of hydrochloric acid to liberate the combined carbon dioxide. The latter solutions were carefully prepared using fresh, cooled solutions, magnetically stirred, in closed vessels with very little free air space. In the first method, with simple barium hydroxide precipitation and back titration, results were generally 3% in error. Using the method of Hammerton and Garner [8], in which the carbon dioxide is precipitated with barium hydroxide, boiled, filtered, and the filtrate and precipitate titrated separately, the results were systematically high by about 10%. In the method of Emmert and Pigford [6], where the carbon dioxide is precipitated with a mixture of barium chloride and sodium hydroxide solution, and the excess sodium hydroxide titrated *in situ*, the average error was less than 2%, and this method was used in the subsequent work.

(c) *Equilibrium Data*—The data for carbon dioxide was taken from I.C.T. [10], and other references quoted by Seidell [15]. The data for ammonia came from Morris and Jackson [12]. In calculating driving force the assumption was made that the gas was dry at the inlet and of 100% humidity at the outlet.

(d) *Discs*—The discs used by previous investigators [1, 5, 11, 13, 14, 17, 18] and the authors have all been approximately of the same dimensions, and it is apparent that, if the number of mixing zones per unit area of absorption surface is increased, the absorption coefficient may well increase. In calculating the absorption surface the convention of S. and M. was used; the total dry surface of the discs was taken with no allowance for points of contact or film thickness.

For the systems used, a column of sixty discs is considered to be a satisfactory compromise to minimize both those errors arising from possible end-effects and those arising from the approach of exit liquor to equilibrium composition.

De-wetting of the liquid on the discs has been reported by a number of investigators, and in some cases the de-wetted areas have been quite extensive, even at flow rates up to 200 lb/hr ft [3]. Although loss of absorption surface will cause low absorption coefficients, the increased flow rates in the wetted areas will tend to offset this, and it is possible that partial de-wetting might give rise to either high or low results. The authors found that, with careful cleaning of the apparatus and submersion of the discs in water between runs, no extensive de-wetting took place. With the Doulton discs (smooth, unglazed, ceramic), the rough sandstone disc, and the smooth pyrophyllite discs, the segments of the faces between 1 and 2 o'clock and 11 and 10 o'clock tended to be starved of liquid at flow rates below 200 lb/hr ft. The set of pyrophyllite discs was roughened systematically by putting a series of criss-cross cuts on the faces and sides (Fig. 1a), in the expectation of creating further turbulence in the liquid film, and consequently higher coefficients. In fact no increase in coefficients was obtained, but the wetting of the discs was so improved that the discs wetted completely at rates below 45 lb/hr ft.

VOL. 5 1956

Nomenclature

D = absolute diffusion coefficient, sq. ft/hr

K_G = over-all absorption coefficient, lb/(hr) (sq. ft) (atm)

k_G = gas-film coefficient, lb/(hr) (sq. ft) (atm)

k_L = liquid-film coefficient, lb/(hr) (sq. ft) lb/cu. ft

n = power to which Re is raised in Sherwood and Holloway's equation.

Re = Reynolds number

v = relative linear velocity of gas and liquid streams, ft/sec

v_G = velocity of gas stream, ft/sec

α = empirical constant obtained by calibration of column, for liquid-film coefficient, ft^{-1}

Γ = liquid flow rate per unit width of surface, lb/(hr) (ft)

ρ = density of gas or liquid, (lb/cu. ft)

μ = viscosity of gas or liquid (lb mass/ft hr)

References

[1] Andrew, S. P. S.; *Chem. Eng. Sci.* **3** 1954 279.

[2] Cooper, C. M., Drew, T. B. and McAdams, W. H.; *Trans. Amer. Inst. Chem. Eng.* 1934 **30** 158.

[3] Danckwerts, P. V. and Kennedy, A. M.; *Trans. Inst. Chem. Eng.* Symposium on Gas Absorption 1954 **32** Suppl. 1. S.58.

[4] Dukler, A. E. and Bergelin, O. P.; *Chem. Engng. Prog.* 1952 **48** 557.

[5] Eldridge, K. P.; Private Communication.

[6] Emmert, R. E. and Pigford, R. L.; *Chem. Engng. Prog.* 1954 **50** 87.

[7] Grimley, S. S.; *Trans. Inst. Chem. Engrs.* 1945 **23** 228.

[8] Hammerton, D. and Garner, F. H.; *Trans. Inst. Chem. Engrs.* Symposium on gas absorption, 1954 **32** Suppl. 1. S.18.

[9] HOFTYZER, P. J. and VAN KREVELEN, D. W.; *Trans. Inst. Chem. Engrs.*, Symposium on gas absorption, 1954 **32** Suppl. 1. S.66.

[10] *International Critical Tables* **3**, 260. McGraw-Hill, New York.

[11] MORRIS, D. R., Ph.D. Thesis, University of London, 1954.

[12] MORRIS, G. A. and JACKSON, J.; *Absorption Towers.* Butterworth 1953.

[13] ROPER, G. H.; *Chem. Eng. Sci.* 1953 **2** 18.

[14] ROPER, G. H.; *Chem. Eng. Sci.* 1953 **2** 247.

[15] SEIDELL, A.; *Solubilities of Inorganic Compounds*, Vol. I, p. 221., 3rd. Edn., Van Nostrand Co., New York, 1940.

[16] SHERWOOD, T. K. and HOLLOWAY, F. A. L.; *Trans. Amer. Inst. Chem. Engrs.* 1940 **36** 39.

[17] STEPHENS, E. J. and MORRIS, G. A. (referred to as "S. and M."); *Chem. Engng. Prog.* 1951 **47** 232; also see SHERWOOD, T. K. and PIGFORD, R. C.; *Absorption and Extraction.* McGraw-Hill, New York, 1952.

[18] WARNER, N. A.; *Chem. Eng. Sci.* 1954 **3** 77.

OL.
5
956

Chemical Engineering Science, 1956, Vol. 5, pp. 178 to 187. Pergamon Press Ltd.

Design calculations for batch distillation column

J. P. W. Houtman* and Asghar Husain

Laboratory of Chemical Engineering, University of Indonesia, Bandung

(*Received* 6 *October*, 1955)

Abstract—The equation developed by Zuiderweg [3], relating sharpness of separation in batch distillation to number of theoretical plates, reflux ratio, and holdup of the column, has been analysed. Based upon this, a method is suggested to choose the most useful combination of number of theoretical plates, reflux ratio, and holdup, in order to obtain a required separation. A nomograph is provided to simplify the calculations. Directions are given for selecting the best column out of the available ones, or for adjusting the amount of charge in case only one column is available.

Résumé—On analyse l'équation développée par Zuiderweg [3] en indiquant le rapport entre l'exactitude de séparation dans la distillation discontinue d'une part et le nombre de plateaux théoriques, le rapport du reflux et le séjour dans la colonne d'autre part. En se basant sur ce qui précède, on propose une méthode pour choisir la combinaison la plus utile du nombre de plateaux théoriques, du rapport de reflux et du séjour afin d'obtenir la séparation requise. Ensuite on donne une nomographie pour simplifier les calculs. Sont données encore des directives pour choisir la meilleure des colonnes disponibles ou de mettre au point la quantité de la charge en cas qu'il n'y ait qu'une seule colonne de disponible.

VOL. 5 1956

Introduction

The calculation of distillation conditions necessary to obtain a required separation of a mixture in batchwise fractionation has been the subject of intensive study.

The phenomenon of continuous change, occurring with time in compositions of liquid and vapour at different places in the column, is more complicated when the amount of holdup is appreciable compared to the charge.

In such cases, which are commonly encountered in practice, the concentration of lower boiling component in the bottom-liquid is markedly reduced due to uptake of material in the column, having a different average composition. Consequently, the concentration of lower boiling becomes smaller in distillate than for the case (theoretical) when holdup is not present. However, this influence on the distillation curve is partly compensated because of the fact that the distillate obtains its components by changing compositions of both bottom-liquid and holdup.† The final result, known as "depletion effect," varies continuously during distillation, and has a detrimental effect upon separation.

Further, it is clear that the change in compositions of liquid and vapour streams by the time-consuming exchange of constituents will be smaller when more of these phases are present. As a result, approach to liquid-vapour equilibria throughout the column is hampered by the presence of holdup. This so called "inertia effect" (or flywheel or hangover effect) prevents quick adjustment of liquid and vapour concentrations in the column in accordance with continuously decreasing concentration of the bottom. It also changes during the course of distillation, and has a beneficial influence upon separation.

Thus the exact mathematical treatment of

* Present Address: Johann Keplerstraat 15, Amsterdam-O.

† The compensating effect is clearly indicated by making a material balance, in which holdup must be included. For that reason operating line in the McCabe-Thiele diagram becomes curved.

these intricate phenomena is possible only by means of a number of differential equations, covering changes in concentration from place to place within the column and with time. PIGFORD and co-workers [1] solved these equations using a differential analyser, and applying certain approximations in order to make the equations adaptable to the instrument. Such an analyser, however, is not available to the average engineer.

ROSE and associates [2] applied a discontinuous method, in which incidental plate-to-plate calculations are done for small time-intervals. This is possible without any specially designed calculator, but the work is so laborious that it is desirable to use a desk-calculator or punched-card machine. Moreover, such calculations can be carried out only for columns containing a limited number of plates.

Further, both methods, mentioned above, enable us only to compute the distillation curve and, out of that, sharpness of separation for a given set of conditions. Whereas the reverse solution, important from the industrial point of view, is only possible by a laborious trial and error method [2].

Recently, ZUIDERWEG [3] developed a comparatively simple equation (1) based on the concept of " pole-height," which was introduced earlier by BOWMAN and CICHELLI [4].

$$\frac{1}{S} = \frac{8}{E}\left[1 + \frac{H}{W_s}\left(\frac{E}{4{\cdot}6 \log E} - 1\right)\right] + \frac{1}{cR(\alpha - 1)\left(1 + 3\,\frac{H}{W_s}\log E\right)} \qquad (1)$$

The usefulness of this equation depends upon the relation between $(dx_D/dW)_{x_D = 0{\cdot}5}$ and the amount of intermediate fraction within limits of certain purity.

$$(dx_D/dW)_{x_D = 0{\cdot}5} \cdot I_{0{\cdot}90 - 0{\cdot}10} = 1{\cdot}18 \qquad (2)$$

$$(dx_D/dW)_{x_D = 0{\cdot}5} \cdot I_{0{\cdot}95 - 0{\cdot}05} = 1{\cdot}70 \qquad (3)$$

$$(dx_D/dW)_{x_D = 0{\cdot}5} \cdot I_{0{\cdot}99 - 0{\cdot}01} \approx 6{\cdot}0 \qquad (4)$$

According to these equations $(dx_D/dW)_{x_D = 0{\cdot}5}$ can be equal to 3, 10, and 20 for poor, normal, and sharp separations respectively.

The application of equation (1) is limited to those cases when relative volatility can be assumed constant over the range considered, and when a sharp separation of components is desired. The latter condition is indispensable, since in that case only W_s can be substituted by a known value, equal to molefraction of higher boiling component in the charge*.

The equation (1) is based partly on scientific reasoning, partly upon experimental evidence. Therefore, it takes into account the depletion and inertia effects of the holdup. It has been checked experimentally, using glass plate columns (Oldershaw type), and further by comparison with the results by PIGFORD. An agreement generally within 10% of the value of $(dx_D/dW)_{x_D = 0{\cdot}5}$ has been reported. The solution of the equation is facilitated by the use of nomographs.

This equation enables one to calculate necessary R in order to attain a certain sharpness of separation (expressed in terms of I or $(dx_D/dW)_{x_D = 0{\cdot}5}$) for given values of N and H. But such information is only useful when a column of known characteristics is already available. On the other hand, what is more interesting to the design engineer is to know the best combination of variables N, R and H for obtaining desired separation.

The present paper treats ZUIDERWEG's equation critically, and suggests a method to meet such requirements.

ANALYSIS ZUIDERWEG'S METHOD

The equation (1) is a unique relation, so far developed, combining all the variables (α, N, R, H, W_s) which influence sharpness of separation in batch distillation. But being quite complicated it does not yield to an easy analysis. Therefore, in order to have a better insight, it seems useful to calculate sharpness of separation at different values of each variable, and plot

* ZUIDERWEG has further shown that, in order to obtain a representative distillation curve, the course of distillation must not be influenced by the starting procedure at total reflux, which is usually applied. For that reason the amount of lower boiling in the charge should not be under twice the amount of holdup.

the results in the form as presented in Figs. 1 and 2†.

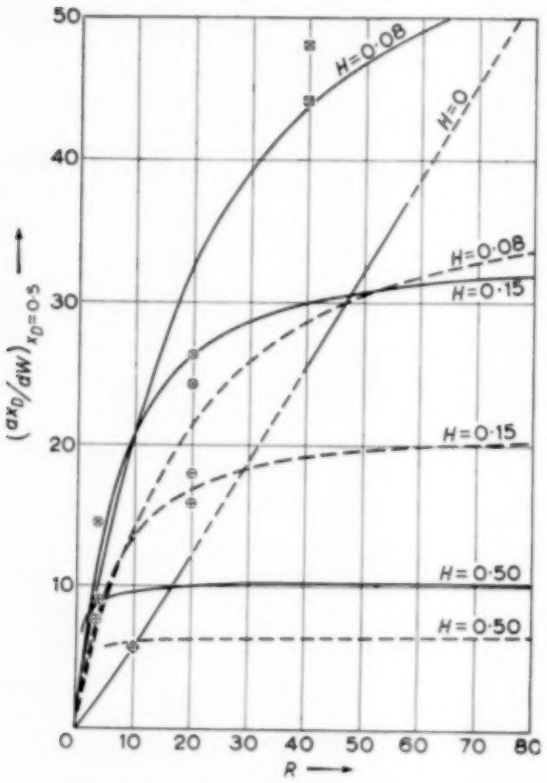

Fig. 1.

Fig. 1 facilitates comparison of equation (1) with the results obtained by other workers [1, 4, 5, 6] who have shown the presence of a "critical reflux ratio," below which holdup is beneficial and above which it is detrimental for separation. In Fig. 1 this critical reflux ratio is represented by the intersection of each curve with the curve for $H = 0$. It is further clear that $R_{cri.}$ depends upon the holdup for particular values of α and N. This was, however, not noted by the previous investigators, but a close examination of their data points to the fact.

From the practical point of view, Fig. 2 is more important, representing sharpness of

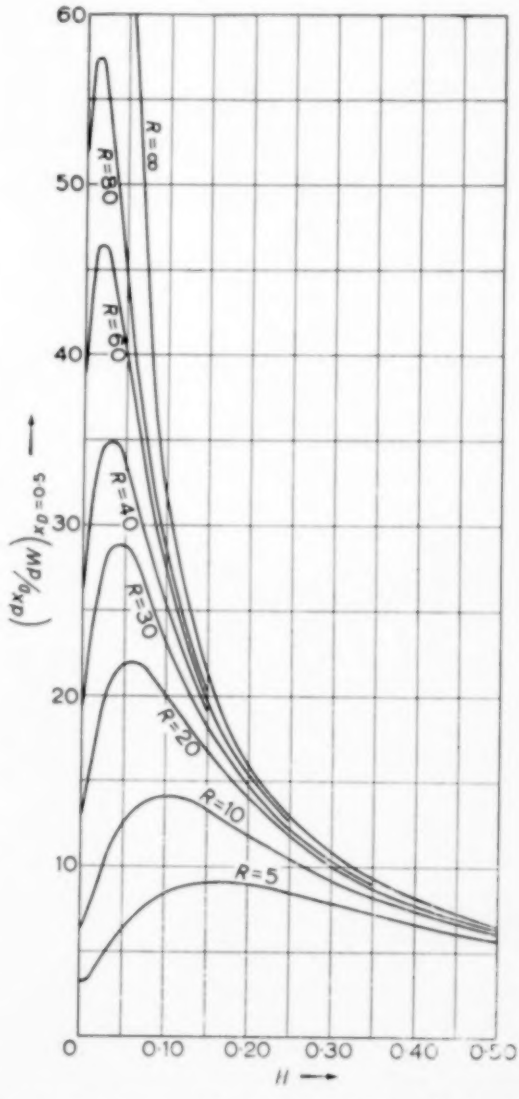

Fig. 2. Cyclohexane *n* heptane ($\alpha = 1{\cdot}65$) equimolecular mixture, $N = 25$.

† In fact graphs similar to Fig. 1 and 2 have already been given by Zuiderweg [3]. But they have been recalculated here, as the original ones seem to contain some mistakes. In Fig. 1 some experimental data as given by Zuiderweg are replotted, indicating validity of equation.

separation versus H with R as parameter. It shows that for each value of R there exists a critical holdup, which gives sharpness of separation equal to that given by zero holdup. Between $H_{cri.}$ and $H = 0$ an optimum holdup provides maximum separation with the same R. Further, it is also clear that a certain value of S can only be obtained with a holdup below a certain maximum.

In short, for a particular desired separation the following holdup values are important for consideration.

(a) Maximum allowable holdup : provides the desired separation with $R = \infty$.

A relation for this can be obtained by substituting $R = \infty$ in equation (1). Solving for H/W_s gives,

$$\frac{H_{max}}{W_s} = \frac{0{\cdot}575\,(E - 8\,S)\log E}{S\,(E - 4{\cdot}6\log E)} \qquad (5)$$

(b) Critical holdup : values of H greater than $H_{cri.}$ necessitate higher values of R than the one required when $H = 0$.

For $H = 0$ equation (1) reduces to,

$$\frac{1}{S_{H=0}} = \frac{8}{E} + \frac{1}{cR\,(\alpha - 1)} \qquad (6)$$

By putting $S = S_{H=0}$ (equations (1) and (6))

$$\frac{H_{cri.}}{W_s} = \frac{4{\cdot}6\;E\log E}{8\,cR(\alpha-1)\,(E-4{\cdot}6\log E)} - \frac{1}{3\log E} \qquad (7)^*$$

Substitution of R from equation (1) gives

$$\frac{H_{cri.}}{W_s} = \frac{0{\cdot}575\,E\log^2 E - \frac{1}{3}S(13{\cdot}8\log^2 E + E - 4{\cdot}6\log E)}{S\,(E - 4{\cdot}6\log E)\log E} \qquad (8)$$

(c) Optimum holdup : provides the required separation with minimum R. It falls between $H_{cri.}$ and $H = 0$.

An equation for $H_{opt.}$ can be derived by differentiating equation (1) with respect to H holding all other variables constant, and putting $d/dH \cdot [(dx_D/dW)_{x_D = 0{\cdot}5}] = 0$. It results into,

$$\frac{H_{opt.}}{W_s} = \sqrt{\frac{4{\cdot}6\;E}{24\,cR\,(\alpha-1)\;(E - 4{\cdot}6\log E)}} - \frac{1}{3\log E} \qquad (9)$$

Substitution of R from equation (1) provides,

$$\frac{H_{opt.}}{W_s} = \frac{0{\cdot}2875E\log^2 E - \frac{1}{6}S(13{\cdot}8\log^2 E + E - 4{\cdot}6\log E)}{S\,(E - 4{\cdot}6\log E)\log E} \qquad (10)^\dagger$$

These characteristic values of holdup, H_{max}, $H_{cri.}$, and $H_{opt.}$, as expressed in relation to α, N and S in equations (5), (8) and (10) seem quite useful in selecting the proper operating conditions for an available column, or for choosing the best out of a number of available columns. This will be discussed in detail in a later part of the paper.

The values of R necessary for the above-mentioned holdups can be found by substituting equations (5), (8) and (10) into equation (1).

It is clear that for H_{max} $R = \infty$. For $H_{cri.}$ the relation for R can be derived directly from equation (6).

$$c\,(\alpha - 1)\,R_{H_{cri.}} = C\,(\alpha - 1)\,R_{H=0} = \frac{SE}{E - 8S} \qquad (11)$$

For optimum holdup R is given by the following equation, obtained from equations (1) and (9).

$$c\,(\alpha - 1)\,R_{H_{opt.}} = \frac{6{\cdot}9\;S^2E\,(E - 4{\cdot}6\log E)\log^2 E}{\left\{S(E - 4{\cdot}6\log E - 13{\cdot}8\log^2 E) + 1{\cdot}725E\log^2 E\right\}^2} \qquad (12)$$

The equation (12) is only valid when the square root of the denominator on the right hand side of the equation is positive.

For simplifying the calculation of R from equations (11) and (12) it is convenient to use a plot of $R\,(\alpha - 1)$ versus $cR\,(\alpha - 1)$, as given in Fig. 3, which has been calculated out of the original plot of c versus $R\,(\alpha - 1)$ given by ZUIDERWEG.

The equation (12) provides the minimum value of R necessary to obtain a desired separation (S) for a particular value of N (α constant). This is represented by a solid curve in Fig. 4, each

* The relation between $R_{cri.}$, α, N, and H/W_s is also given by equation (7). In this case $R = R_{cri.}$ and $H_{cri.} = H$.

† From equations (8) and (10) it is obvious that $H_{opt.} = \frac{1}{2}H_{cri.}$ for the same value of S, which is not the case when both holdups are calculated for the same R (compare equations (7) and (9)).

point of which is related to a value of $H_{opt.}/W_s$ as given by equation (10).

Further, Fig. 4 shows a family of dotted curves, representing equation (1) for different values of H/W_s but at the same α and S. As is obvious from it and also from the theoretical treatment, the solid curve envelopes all the dotted curves. The common point between a dotted curve, valid for a certain value of H/W_s, and the solid line gives the combination of N and R for which that particular H/W_s becomes $H_{opt.}/W_s$. Similarly, the intersection of the same dotted curve with the plot for $H = 0$ provides N and R for which the respective H/W_s is critical.

The mutual relation between Fig. 2 and 4 can be easily traced by moving on a horizontal line on the latter (N constant) in a direction of H/W_s increasing from zero. To obtain the same S (α constant) necessary R decreases until the enveloping curve is reached; further increase in H/W_s necessitates higher R. During the latter course H/W_s passes through the critical value.

In addition to the curves mentioned above, Fig. 4 shows another family of curves (broken lines) which connect equal $H_{opt.}/W_s$ values for different enveloping curves.

A relation for these curves is found by solving S out of equation (10) and substituting it into equation (1).

$$c(\alpha-1)R = \frac{1{\cdot}725\,E\log^2 E}{(E-4{\cdot}6\log E)\left[1+3\left(\frac{H_{opt.}}{W_s}\right)\log E\right]^2} \qquad (13)$$

Due to the large slopes found in these constant $H_{opt.}/W_s$ curves, necessary N changes strongly with increase in S for high values of $H_{opt.}/W_s$.

Selection of N, R and H

For a given α and S the enveloping curve of

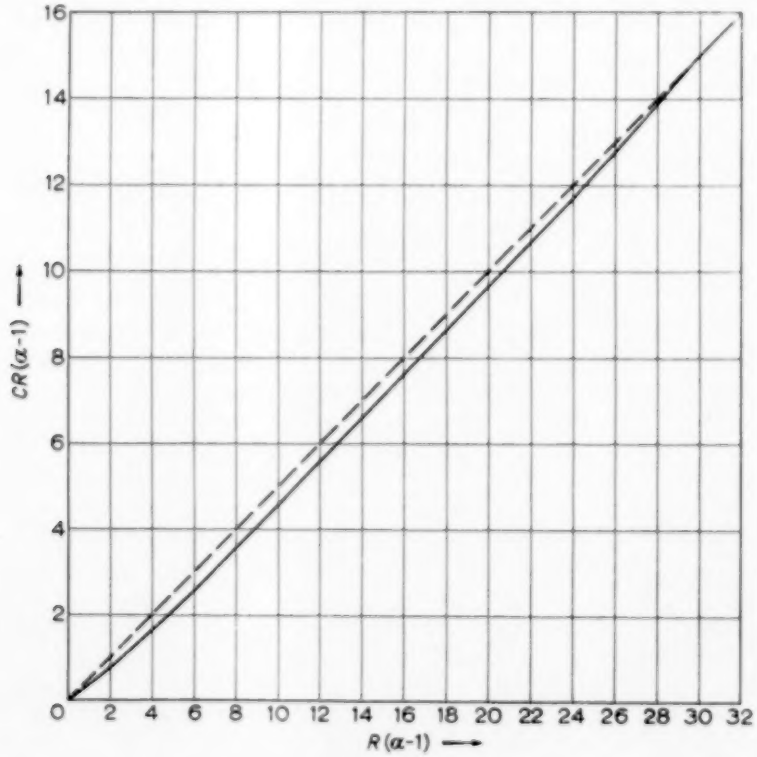

Fig. 3.

VOL. 5 1956

Fig. 4 seems very helpful in choosing the best combination of N, R and H, as it provides lowest R for each value of N.

Any selection of N and R, whatsoever, should not be based only on economic reasons, but also on the possibility of making small adjustment in R when N and H of the column are not completely in agreement with the values obtained in design calculations.

In this connection it is well known that both plate-efficiency and holdup depend on construction factors. Further, plate-efficiency, and in the case of packed columns also holdup, change with operating conditions (flow rates), and properties (i.e. concentrations) of liquid and vapour streams present in the column. Thus the plate-efficiency (or number of theoretical plates actually present in the final column) and holdup cannot be estimated with high accuracy during design; moreover, they can change during operation.

In view of this, the central part of the enveloping curve is very interesting. Here small changes in either N, R or H do not require great changes in the others, particularly for the reason that the deviations between a dotted line (Fig. 4) and the enveloping curve above and below their common point is nearly equal and relatively small when the common point is situated in the central part of the enveloping curve.

For cases when the N-versus-R curve (solid curve, Fig. 4) is more or less symmetrical with respect to the bisector, which appears to be true for not too high values of S*, the best stable

* It is interesting to note that the enveloping curve in Fig. 4 is more or less symmetrical and not the curve for $H/W_s = 0$, as would be expected from data of Rose [7]. In fact there is a discrepancy between equation (1) and the work of Rose. According to Rose, holdup values under 5% of charge have no strong influence on the sharpness of separation, which is not in agreement with Fig. 2. However, there are indications [8] that the conclusion of Rose is not generally true.

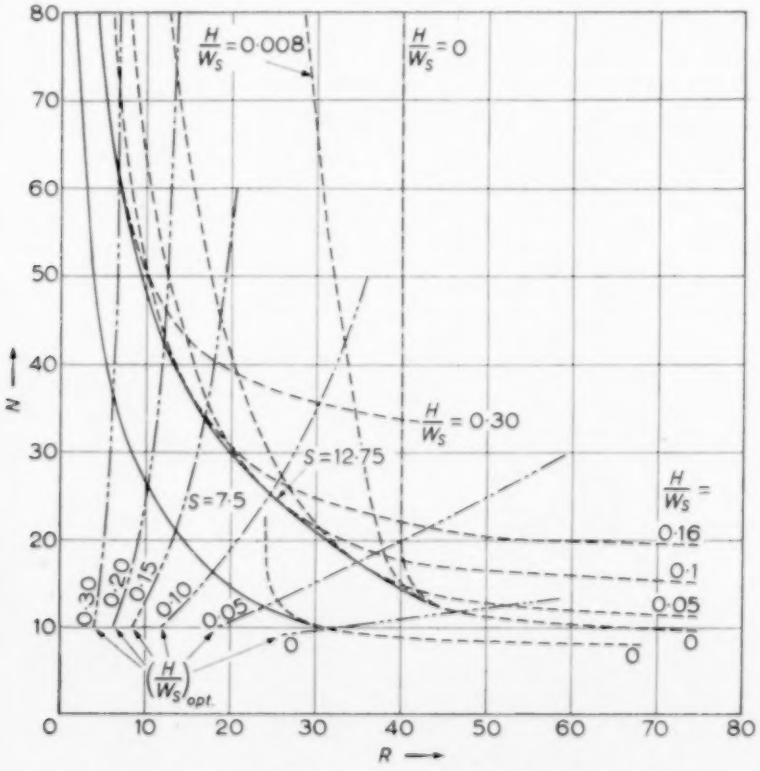

Fig. 4. Relation between N, R and H for $S = 7{\cdot}5$ and $12{\cdot}75$, $\alpha = 1{\cdot}65$.

combination of N and R will be represented by a point lying nearest to the origin. An attempt to derive a relation for these points out of equation (12) by putting $d/dN \cdot [(R^2 + N^2)] = 0$ did not result in a simple mathematical expression. Therefore, an indirect method was used, in which a number of enveloping curves were calculated for different values of α (1·1 — 2·5), $(dx_D/dW)_{x_D=0.5}$ (5 — 20), and W_s (0·4 — 0·7). For each curve the nearest point to the origin was located. As shown in Fig. 5, they fall almost on parallel straight lines each for a different α, independent of W_s and $(dx_D/dW)_{x_D=0.5}$.

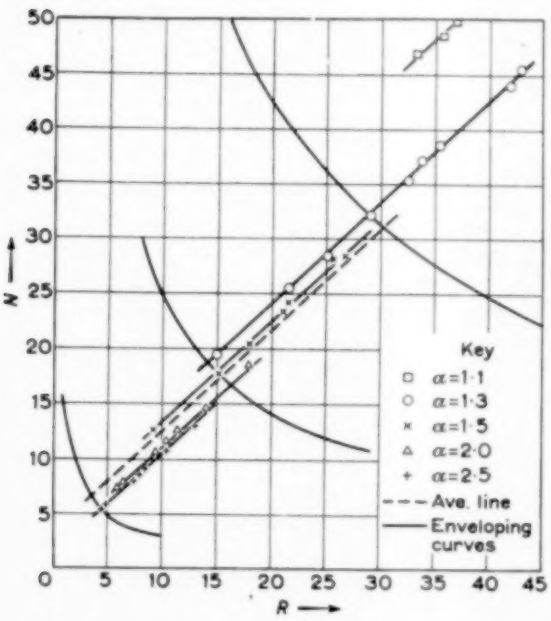

Fig. 5. Nearest points of enveloping curves.

The following equations were deduced for the straight lines.

For $\alpha = 1{\cdot}1$ $N = 0{\cdot}920\ R + 16$ (14)

$= 1{\cdot}3$ $N = 0{\cdot}920\ R + 5{\cdot}75$ (15)

$= 1{\cdot}5$ $N = 0{\cdot}912\ R + 4{\cdot}25$ (16)

$= 2{\cdot}0$ $N = 0{\cdot}909\ R + 1{\cdot}75$ (17)

$= 2{\cdot}5$ $N = 0{\cdot}915\ R + 1{\cdot}25$ (18)

For design purpose an average equation will be sufficient in the normal range of α $(1{\cdot}3 < \alpha < 2{\cdot}5)$.

$$N = 0{\cdot}91^5\ R + 3{\cdot}30 \qquad (19)\dagger$$

Equation (19) when combined with (12) gives equation (20), in which the most useful $N = N_u$ is only a function of α and S.

$$c\,(\alpha - 1)\,(N_u - 3{\cdot}30) = \frac{6{\cdot}307\ S^2\ E\,(E - 4{\cdot}6 \log E)\log^2 E}{\{S(E - 4{\cdot}6\log E - 13{\cdot}8\log^2 E) + 1{\cdot}725\log^2 E\}^2} \qquad (20)$$

in which $E = \alpha^{N_u + 1}$.

The solution of N_u out of equation (20) is very difficult. Therefore, a nomograph, Fig. 6, has been provided for the computation of N_u, and related R and $H_{opt.}/W_s$ (equations (19) and (10)). The use of the nomograph is illustrated by the following example.

Example 1 : A mixture of 35 mole per cent benzene and 65 mole per cent toluene ($\alpha = 2{\cdot}42$) has to be separated into three fractions. The intermediate fraction should contain all the distillate with purity between 5 and 95% benzene, and its amount should be limited to 10 mole per cent of the charge.

From equation (3) $(dx_D/dW)_{x_D=0.5} = 1{\cdot}7/0{\cdot}1 = 17{\cdot}0$

$W_s = 0{\cdot}65$, $S = (0{\cdot}65)\ (17{\cdot}0) = 11{\cdot}05$.

From Fig. 6 diagram A $N_u = 13$

diagram B $R = 10{\cdot}6$

diagram C $\log E = 5{\cdot}32$

diagram D $H_{opt.}/W_s = 0{\cdot}11$

$H_{opt.} = (0{\cdot}11)\ (0{\cdot}65) = 0{\cdot}070$ or 7 mol% of the charge.

Further, the nomograph provided by Zuiderweg can be used for calculating the necessary variation in R if certain deviation (for instance 10%) is assumed in N and H between the actual values and those calculated here.

Separation of Multicomponent Mixtures

Zuiderweg has further shown that the equation (1) is also applicable for multicomponent mixtures if sharp separation is present. Such a distillation can be considered as consisting of a number of binary separations, for each of which there will

† By plotting this average line on Fig. 4, it is clear that for high values of S small H/W_s, and for low values of S large H/W_s are suitable.

VOL. 5 1956

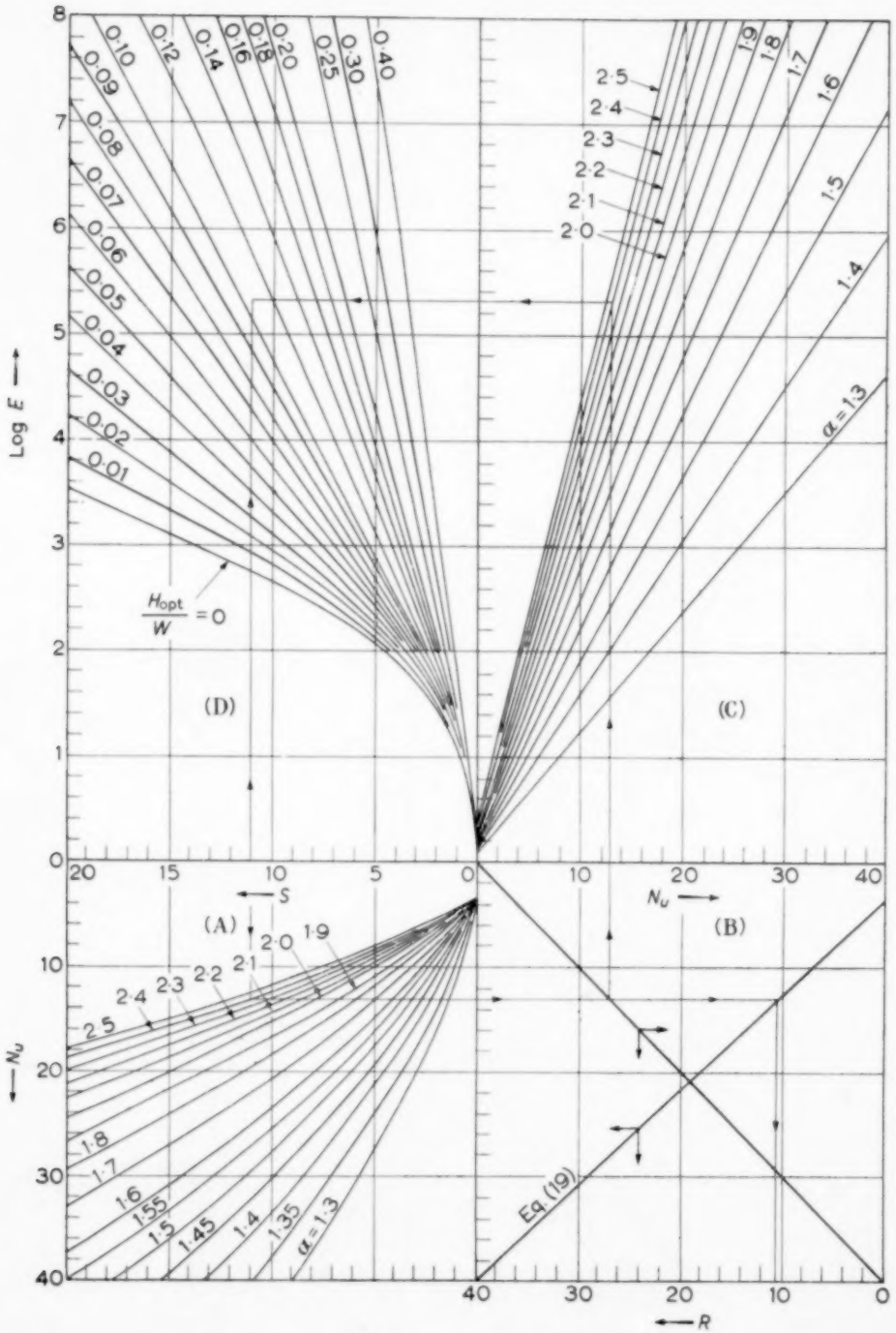

FIG. 6. Nomograph for the solution of N_u, R and H_{opt}.

be a combination of N_u, R and H. In such a case a selection of N and H has to be made out of the different values obtained. Care must be taken that the selected H is not equal to or above H_{max}. For other separations involved, R can be adjusted in each part of the distillation.

Example 2 : A mixture of 20 mole per cent benzene, 50% toluene, and 30% xylene has to be separated so that the intermediate fractions, taken between limits of concentration of respective lower boiling component 0·9 – 0·1 molefraction, should contain 6 mole per cent of the binary mixture under consideration.

Here W_s will be equal to the molefraction of the higher boiling component in each binary separation compared to the total charge. Similarly, I will be molefraction of intermediate distillate in each separation with respect to the charge.

(a) Separation benzene-toluene ($\alpha = 2{\cdot}42$)

$W_s = 0{\cdot}5$, $I = (0{\cdot}06)\ (0{\cdot}70) = 0{\cdot}042$.

From equation 2 : $(dx_D/dW)_{x_D = 0{\cdot}5} = 1{\cdot}18/0{\cdot}042$, and

$S = (1{\cdot}18/0{\cdot}042)\ (0{\cdot}50) = 14{\cdot}05$.

From Fig. 6 diagram A $N_u = 15$

diagram B $R = 12{\cdot}6$

diagram C $\log E = 6{\cdot}02$

diagram D $H_{opt.}/W_s = 0{\cdot}095$

$H_{opt.} = (0{\cdot}095)\ (0{\cdot}50) = 0{\cdot}047$.

(b) Separation toluene-xylene ($\alpha = 2{\cdot}20$)

$W_s = 0{\cdot}3$, $I = (0{\cdot}06)\ (0{\cdot}80) = 0{\cdot}048$

$(dx_D/dW)_{x_D = 0{\cdot}5} = 1{\cdot}18/0{\cdot}048$, and

$S = (1{\cdot}18/0{\cdot}048)\ (0{\cdot}30) = 7{\cdot}375$.

From Fig. 6 diagram A $N_u = 11$

diagram B $R = 8{\cdot}8$

diagram C $\log E = 4{\cdot}23$

diagram D $H_{opt.}/W_s = 0{\cdot}125$

$H_{opt.} = (0{\cdot}125)\ (0{\cdot}30) = 0{\cdot}037$.

Election of R and H/W_s for a certain Column

When the amount of charge is limited, as in most of the laboratory distillations, H/W_s and N will be fixed if a particular column is used. As mentioned before, the required separation is always possible with the proper adjustment of reflux ratio provided that the holdup is lower than $H_{max.}$. Therefore, in such a case a check for $H_{max.}$ is sufficient. But it is more suitable to use a holdup ratio not so near to H_{max}, so that the required separation can still be obtained if for any reason the holdup of the column is increased in actual operation. Moreover, a too-high value of α estimated in the beginning can also annul the possibility of attaining desired separation if H is chosen close to H_{max}. Such a wrong estimation of α is quite possible, because the equations given for its calculation out of boiling points (9) and (10) are only approximations.

If the amount of charge is not limited, as in most technical and some laboratory fractionations, H/W_s for a given column can be adjusted to the optimum value by starting with the proper amount of charge. For such a case (N, α, S fixed) equation (10) or Fig. 6 diagram D can be used to calculate $H_{opt.}/W_s$, and equation (12) for $R_{H_{opt.}}$.

Notation

N = Number of theoretical plates in the column

N_u = Most useful number of theoretical plates in the column

H = Operating holdup as molefraction of charge

$H_{max.}$ = Maximum operating holdup as molefraction of charge

$H_{cri.}$ = Critical operating holdup as molefraction of charge

$H_{opt.}$ = Optimum operating holdup as molefraction of charge

R = Reflux ratio

$R_{H_{cri.}}$ = Reflux ratio used with $H_{cri.}$

$R_{H_{opt.}}$ = Reflux ratio used with $H_{opt.}$

x_D = Molefraction of the lower boiling component in the distillate

W_s = Amount of liquid not yet distilled (material left in the bottom and column) at $x_D = 0{\cdot}5$, as molefraction of the charge

$(dx_D/dW)_{x_D = 0{\cdot}5}$ = Slope of the distillation curve (x_D versus W) at $x_D = 0{\cdot}5$

S = Pole-height = $W_s\,(dx_D/dW)_{x_D = 0{\cdot}5}$

α = Relative volatility

$E = \alpha^{N+1}$

c = A function of $R(\alpha - 1)$ plotted by Zuiderweg (see Fig. 3), for $R(\alpha - 1) > 30$, $c = 0{\cdot}5$

I = Amount of intermediate fractions a molefraction of charge

VOL. 5 1956

References

[1] Pigford, R. L., Tepe, J. B., and Garrahan, C. J., *Industr. Eng. Chem.*, 1951 **43** 2592.

[2] Rose, A., *et al.*, *Industr. Eng. Chem.*, 1940 **32** 673-675 ; 1950 **42** 2145, 2494 ; 1951 **43** 2459, 2502 ; *Chem. Eng. Progress*, 1953 **49** 15.

[3] Zuiderweg, F. J., *Chem. Ing. Techn.*, 1953 **25** 297.

[4] Bowman, J. R., Cichelli, M. T., *et al.*, *Industr. Eng. Chem.*, 1949 **41** 1985 ; 1950 **42** 2502.

[5] Rose, A., *et al.*, *Industr. Eng. Chem.*, 1950 **42** 1876, 2145 ; *Chem. Eng. Progress*, 1952 **48** 549.

[6] Colburn, A. P., and Stearns, R. F., *Trans. Amer. Inst. Chem. Engrs.*, 1941 **37** 291.

[7] Rose, A., *Industr. Eng. Chem.*, 1941 **33** 594.

[8] Rose, A., *et al.*, *Industr. Eng. Chem.*, 1952 **44** 1480.

[9] Weissberger, A., *Technique of Organic Chemistry* : *Vol. IV Distillation*, page 22, Interscience Pub. Inc., New York, 1951.

[10] Carney, Thomas P., *Laboratory Fractional Distillation*, page 41, The Macmillan Co., New York, 1949.

OL.
5
956

Chemical Engineering Science, 1956, Vol. 5, pp. 188 to 192. Pergamon Press Ltd.

The binary system cyclohexane-methyl ketone

M. B. Donald and K. Ridgway

Department of Chemical Engineering University College London

(*Received* 27 *September*, 1955)

Abstract—In an investigation of the ternary close-boiling system benzene-cyclohexane-methyl ethyl ketone, it was found that although vapour-liquid equilibrium data existed for two of the three binary systems, [1, 2], none existed for the cyclohexane-methyl ethyl ketone system. The system was investigated and found to form a minimum-boiling azeotrope at 52·3 mol % cyclohexane and 71·5°C at atmospheric pressure. The following properties were also determined as functions of the composition: refractive index, density, surface tension, viscosity, heat of mixing, and freezing-point. A eutectic occurred at 12·3 mol.% cyclohexane at a temperature of −91°C.

Résumé—Les auteurs, dans leurs recherches sur le système ternaire à point d'ébullition voisin benzène-cyclohexane-methyl-éthyl-cétone, ont trouvé que, bien que l'on possède des données sur l'équilibre liquide vapeur pour deux de ces trois systèmes binaires, pas une n'existait pour le système cyclohexane–methyl-ethyl-cétone. Ils ont étudié ce système qui présente un azéotrope à point d'ébullition minimum (à 52·3 mol %, 71°5C et pression atmosphérique). Ils ont alors déterminé les propriétés suivantes en fonction de la composition : indice de réfraction – densité – tension superficielle – viscosité – chaleur de mélange – point de congélation. Ils ont trouvé un eutectique pour une composition de 12·3 % molaire de cyclohexane à une température de −91°C.

Purification of Materials

(1) *Methyl ethyl ketone*

The substance as supplied by the manufacturers was dried over calcium chloride, then over pellet caustic soda, and was distilled through a three-foot gauze ring packed column, collecting the central fraction. The boiling-point of the fraction was 79·45°C to 79·55°C, and the physical properties showed it to be a pure material :

Refractive index, $n_D^{25} = 1{\cdot}3761$ (lit. value, 1·37612 ; ref. 3).

Density at 25°C, gm/ml = 0·7999 (lit. value, 0·80020 ; ref. 3).

(2) *Cyclohexane*

Pure cyclohexane from the manufacturers was found, by determination of its ultra-violet spectrum, to contain about 0·2% of benzene ; it was therefore refluxed for six hours with mixed nitric and sulphuric acids, washed several times with aqueous sodium carbonate solution to remove acid, and distilled through the column to remove the nitrobenzene into which the benzene originally present had been converted. Re-determination of the ultra-violet absorption showed that the benzene bands were now completely absent. The product used distilled entirely within 0·05°C of the published boiling-point of 80·8°C, and had the physical properties :

Refractive index $n_D^{25} = 1{\cdot}4233$ (lit. value, 1·42354 ; ref. 3).

Density at 25°C, gm/ml = 0·7737 (lit. value, 0·77389 ; ref. 3).

Experimental

The refractive index and density of the mixtures were measured primarily to afford a method of analysis in the determination of the vapour-liquid equilibrium.

Refractive index was determined by means of a Hilger Abbe-type refractometer reading directly in refractive index to 0·0001, thermostatted at 25°C ± 0·02°C by water circulated by a small centrifugal pump. This gave an accuracy of 1 part in 400 on the analysis.

Densities were determined in glass Sprengel-Ostwald pyknometers of approximately 6 ml capacity, fitted with ground-on stoppers to prevent evaporation during

weighing. Weighings were carried out on a semi-micro direct-reading balance on which 0·1 mg could be read directly, and 0·02 mg estimated. Densities were corrected to vacuo, and were reproducible to better than 0·0001 gm/ml. Curves of refractive index and density versus composition were constructed by measuring the properties of mixtures of known composition prepared by weighing into weighing bottles fitted with ground-on stoppers to prevent evaporation.

The vapour-liquid equilibrium was determined in a Pyrex still of the type described by GILLESPIE [4], but having the liquid down-comer from the separating chamber interrupted by a U-tube to hold a liquid sample as recommended by FOWLER [5]. The Cottrell lift was lagged with asbestos rope over a Nichrome heating coil arranged to supply sufficient heat to keep the lift at 80°C with the still empty, as measured by a thermocouple in contact with the glass. The boiling equilibrium temperature in the separating chamber was measured by a mercury-in-glass thermometer reading to $\frac{1}{10}$°C. Samples from the condensate and liquid traps, and from the boiler, were drawn, whilst the still was running, into weighing bottles stoppered to prevent evaporation, after an equilibrating time of three hours. The refractive indices of the contents of the boiler and the liquid trap agreed in all cases to 0·0002, indicating that, in this smooth-boiling, completely miscible system, the boiling liquid and the evolved vapour were substantially in equilibrium at the point of production. The pressure in the still was kept at 760 mm of mercury by blowing in or extracting air as required from the ambient pressure, through a Marriotte bottle and a 50-litre carboy to iron out momentary pressure fluctuations.

The surface tensions were measured by a torsion balance which determined the force necessary to detach a small platinum wire ring from the surface of the liquid. The instrument was calibrated by means of a number of pure organic liquids, and found to have a scale reading which was linear with the surface tension over the range of measurement utilized (16 to 30 dynes/cm). In each determination the mean of five measurements was taken, all of which agreed to 0·2 dyne/cm.

Viscosities were measured in an Ostwald viscometer conforming to B.S.S. 188, No. 2. It was suspended in a thermostat at 25°C ± 0·02°C and calibrated with distilled water, which had an efflux time of 144 seconds.

The heats of mixing of the two liquids were measured in a calorimeter similar to that used by VOLD [6], consisting of a wide-mouthed Dewar vessel. The vessel was closed by a large cork, through which passed a glass stirrer driven at a constant speed by an electric motor, a Beckmann thermometer reading to 0·005°C, a pipette to contain one of the pure components to be added to a mixture in the body of the calorimeter, and a small nichrome heating coil wound on a glass tube. The pipette (Fig. 1) held 25 ml of one of the pure liquids, kept separate from the remaining liquid by the bend in the capillary tube *A*. It was discharged by blowing air into the conical

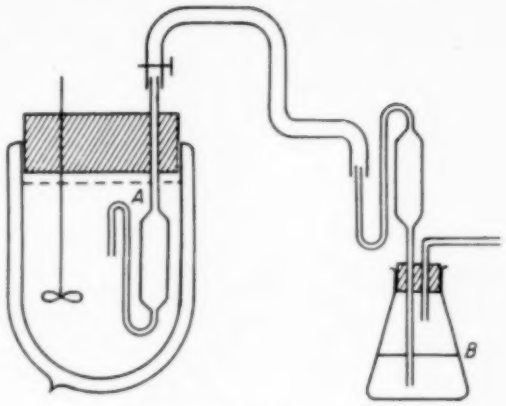

FIG. 1.

flask *B* until the water just filled the duplicated pipette dipping into the flask, thus enabling the contents of the pipette in the calorimeter to be discharged without the fear of any excess air being blown through the liquid mixture and causing a cooling effect by evaporation. The free space below the lid was only 35 ml, in comparison with a calorimeter charge of 350 ml, so that the correction due to the change in composition of the vapour on mixing the liquids was negligible. The calorimeter was heated after each run by the 47-ohm nichrome coil. The voltage across a 0·6-ohm standard resistance in series with the coil was measured by a potentiometer to obtain the total electrical energy supplied, and a heating carried out after each mixing to give the thermal capacity of the arrangement under the conditions used. The charge to the calorimeter was accurately made by a 350 ml pipette.

Freezing-point curves were determined by cooling mixtures of various compositions in a boiling tube jacketted by a larger tube, the two being dipped into a liquid nitrogen bath, and temperature readings made every thirty seconds. The mixture was stirred as long as possible with an electrically-driven vertical stirrer. A copper-constantan thermocouple whose cold junction was in the mixture tube and whose hot junction was kept at 100°C by boiling distilled water, suspending the junction in the steam, measured the temperature of the cooling mixture. The couple was calibrated with various pure organic liquids whose freezing points lay between 10°C and − 120°C. The e.m.f. was measured to 1 microvolt. Specimens took from 15 to 20 minutes to cool from room temperature to − 80°C.

RESULTS

Table 1 shows the values of the refractive indices, densities and viscosities of cyclohexane-methyl ethyl ketone mixtures at rounded values of molar fraction.

Table 1.

Molar fraction cyclohexane	*Density at 25°C gm/ml*	*Refractive index* n_D^{25}	*Viscosity at 25°C centipoises*
0·0	0·7999	1·3761	0·396
0·1	0·7943	1·3798	0·410
0·2	0·7893	1·3838	0·425
0·3	0·7852	1·3882	0·444
0·4	0·7820	1·3927	0·472
0·5	0·7791	1·3977	0·508
0·6	0·7756	1·4026	0·548
0·7	0·7745	1·4074	0·595
0·8	0·7732	1·4129	0·665
0·9	0·7729	1·4182	0·752
1·0	0·7737	1·4233	0·889

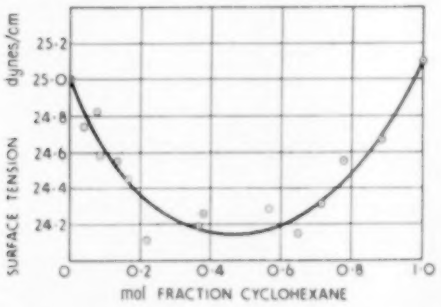

Fig. 2 is a plot of surface tension at 16°C against molar composition. The published values of the surface tensions of methyl ethyl ketone and cyclohexane at this temperature are 24·97 and 24·81 dynes/cm respectively, compared with the experimental values of 25·0 and 25·1 dynes/cm.

The quantity of heat absorbed on adding one gram of either pure component to mixtures of various compositions is shown in Table 2.

The curve showing the total heat absorbed on making a mixture of any given composition at 18°C from the pure components is shown in Fig. 3.

The upper and lower arrest points on the cooling curves of the mixtures yielded a typical binary

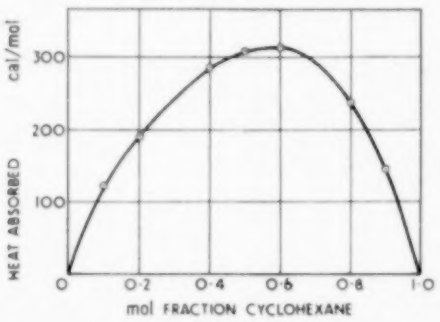

Fig. 3.

Table 2.

Molar fraction cyclohexane	*Heat absorbed, cal/gm cyclohexane added*	*Molar fraction cyclohexane*	*Heat absorbed, cal/gm methylethyl ketone added*
0·025	13·71	0·124	0·41
0·095	12·04	0·238	0·87
0·193	10·05	0·381	1·45
0·400	6·84	0·491	2·96
0·485	5·49	0·598	4·96
0·614	3·62	0·797	10·05
0·783	1·60	0·895	14·26
0·875	1·08	0·958	22·03

25 ml pure component in 350-ml mixture

VOL. 5 1956

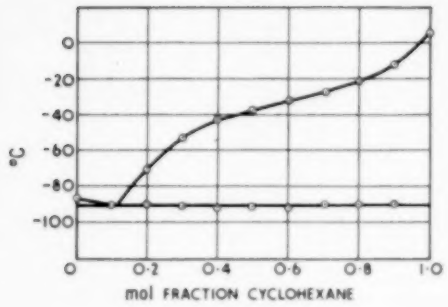

FIG. 4.

eutectic diagram. The interpretation of the cooling curves was complicated by the fact that cyclohexane has a transition point in the solid state at − 89°C, which is very close to the melting point of methyl ethyl ketone at − 87·3°C. The solid-liquid phase diagram is shown in Fig. 4.

The vapour-liquid equilibrium data are given in Table 3. The system forms a binary azeotrope at 52·3 molar per cent. of cyclohexane, boiling at 71·5°C.

As a check of the azeotropic composition, a cyclohexane-rich and a methyl ethyl ketone-rich mixture were each boiled up the column used to purify the materials. Both gave an overhead with $n_D^{25} = 1{\cdot}3988$, or 52·3 molar per cent. cyclohexane, showing that this most volatile mixture occurred at the same point as that at which the x-y plot crossed the diagonal.

The thermodynamic consistency of the vapour-liquid equilibrium results has been checked by the modification of the Herington [7] method suggested by THIJSSEN [8]. According to this method, liquid mixtures whose vapours obey the ideal gas laws obey the equation :

$$\int_0^1 \left(\frac{-\Delta L}{RT^2} \cdot \frac{dT}{dx}\right) dx + \int_0^1 \ln \frac{\gamma_1}{\gamma_2}\, dx = 0$$

where ΔL is the integral heat of mixing per mole of mixture, R is the gas constant, T the absolute temperature, x the molar fraction of one component, and γ_1 and γ_2 are the two activity coefficients. A graph of $\ln \frac{\gamma_1}{\gamma_2}$ against the molar fraction of cyclohexane in the liquid phase should

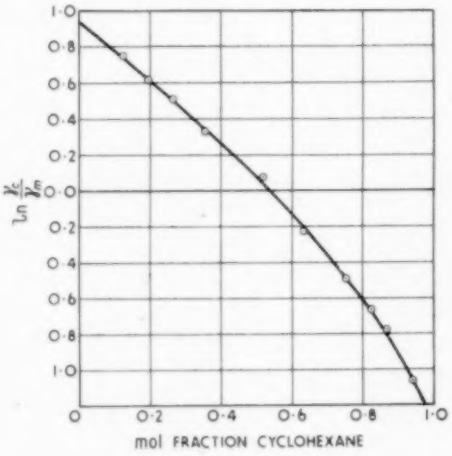

FIG. 5.

Table 3.

Molar fraction cyclohexane		*Boiling temp., C*	$\ln \gamma_{cyclo}$	$\ln \gamma_{mek}$	$\ln \frac{\gamma_{cyclo}}{\gamma_{mek}}$
Liquid	*Vapour*				
0·124	0·223	75·3	0·760	0·013	0·747
0·196	0·302	74·0	0·643	0·025	0·618
0·264	0·366	73·0	0·569	0·062	0·507
0·355	0·426	72·1	0·457	0·127	0·330
0·520	0·535	71·5	0·304	0·229	0·075
0·631	0·580	71·8	0·152	0·380	− 0·228
0·753	0·644	72·6	0·098	0·590	− 0·492
0·825	0·701	73·7	0·060	0·722	− 0·662
0·869	0·747	74·7	0·038	0·811	− 0·773
0·940	0·836	77·0	0·002	1·08	− 1·08

thus give a curve crossing the $\ln \frac{\gamma_1}{\gamma_2} = 0$ line, and cutting off equal areas above and below it. This plot is shown in Fig. 5. Planimeter measurement showed the two areas to agree to within 3%. The term $\frac{-\Delta L}{RT^2} \cdot \frac{dT}{dx}$ is negligible, its value being 0·02 at 0·25 molar fraction cyclohexane. The results are thus consistent assuming vapour-phase ideality, to test which would require a knowledge of the virial coefficients.

Conclusions

The expansion in volume and absorption of heat on mixing, and the lowering of the surface tension show the inter-molecular attractive forces in the mixture to be less, between unlike molecules, than the geometric mean of those between the two types of like molecules. The freezing point curve shows the inflected shape to be expected for a substance such as cyclohexane, which has a practically spherical molecule, and for which $\frac{\Delta_f h}{RT} < 2$, and therefore for which $\frac{\partial^2 T}{\partial x^2} > 0$ [9], where $\Delta_f h$ is the molar latent heat of fusion at temperature T, and R is the gas constant.

This work has been carried out as part of an investigation of the benzene-cyclohexane-methyl ethyl ketone ternary system, the results of which will be published in due course.

Acknowledgements—Our thanks are due to the Salters' Institute of Industrial Chemistry for the generous provision of an ultra-violet absorption spectrophotometer and a refractometer, and to Albright & Wilson, Ltd., Birmingham, for the award of a research grant.

VOL. 5 1956

References

[1] Richards and Hargreaves, *Industr. Engng. Chem.*, 1944 805.

[2] Steninhauser and White, *Industr. Engng. Chem.*, 1949 2912

[3] Dreisbach, *Physical Properties of Organic Compounds*, tables compiled for the Dow Chemical Company.

[4] Gillespie, *Industr. Engng. Chem. (Anal.)*, 1946 **18** 575.

[5] Fowler, Ph.D. Thesis, University of London 1949, also *J. Soc. Chem. Ind.*, 1949 **68** 131.

[6] Vold, J. A. C. S., 1937 **59** 1515.

[7] Herington, *Trans. Faraday Soc.*, 1948 **44** 629.

[8] Thijssen, *Chem. Eng. Sci.*, 1955 **4** 75.

[9] Prigogine and Defay, *Chemical Thermodynamics*, p. 361. (Longmans).

Chemical Engineering Science, 1956, Vol. 5, pp. 193 to 197. Pergamon Press Ltd.

Ueber das Verdampfungsgleichgewicht des Systems Wasser—Pyridin

VON N. IBL, G. DÄNDLIKER UND G. TRÜMPLER

Laboratorium für physikalische Chemie und Elektrochemie der Eidg. Techn. Hochschule, Zürich, Schweiz.

(*Received 14 September, 1955*)

Abstract—The vapour-liquid equilibrium of the system water-pyridine has been studied at constant temperature (50° and 30°C) by a static and by a dynamic method. The results obtained by both methods were in good agreement.

The composition of the azeotropic mixture showed no significant change with temperature between 30° and 80°C. Although the composition of the azeotrope is about one mole of pyridine to three moles of water, no such compound exists in the vapour phase, as was shown by vapour density measurements.

Résumé—L'équilibre liquide-vapeur du système eau-pyridine a été étudié à température constante (50° et 30°C). Les résultats obtenus par une méthode dynamique sont en bon accord avec les mesures faites par une méthode statique.

L'azéotrope n'est pas sensiblement influencé par la température entre 30° et 80°. Quoique la composition du mélange azéotropique soit assez exactement d'une molécule de pyridine pour trois molécules d'eau, il n'existe pas de combinaison correspondant à cette formule dans la phase gazeuse, ce qui a été montré par la détermination de la densité de vapeur.

1. EINLEITUNG

Das Verdampfungsgleichgewicht des Systems Wasser-Pyridin ist wegen seiner technischen Bedeutung sowie wegen seinen starken Abweichungen vom idealen Verhalten wiederholt untersucht worden[1–8]. Die Versuchsergebnisse stimmen jedoch zum Teil schlecht miteinader überein[6]. Als Ergänzung einer früheren Mitteilung[6] wurde in der vorliegenden Arbeit das Dampfdruck diagramm des Systems Wasser-Pyridin nach zwei Methoden (statisch und dynamisch) bestimmt und die Ergebnisse miteinander verglichen.

2. UNTERSUCHUNGSMETHODE*

a. Apparatives.

Die bei der dynamischen Methode verwendete Anordnung ist bereits früher beschrieben worden[6].

Die statische Apparatur (Fig. 1) entspricht im wesentlichen der von Kortüm[9] benützten Anordnung. Das zu untersuchende Gemisch wird zunächst entgast, indem es im Kölbchen K mit einer Azeton-Kohlensäureschne Mischung zum Erstarren gebracht und unter Vakuum gesetzt wird. Hierauf wird das Gemisch wieder aufgetaut und die Operation mehrmals wiederholt. Das Kölbchen wird dann bei geschlossenem Hahn A durch Oeffnen von D mit dem Dampfraum I von ca. 5 Liter Inhalt in Verbindung gesetzt, die Apparatur bis zu den Hahnen A und B in ein Wärmebad getaucht und dieses allmählich auf die gewünschte Temperatur aufgeheizt. Das Quecksilber im Zwischenmanometer M steuert über die elektrischen Kontakte 1 und 2 mit Hilfe eines Magneten E den in Quecksilber eintauchenden Eisenkern K, wodurch die Fritte F solange freigegeben wird und Luft in den äussern Schenkel des Zwischenmanometers M einlässt, bis der Druck im äusseren Schenkel und im Dampfraum I gleich ist. Der Druck kann dann an einem Spiegelskalamanometer ausserhalb des Thermostaten auf 0·1 mm genau abgelesen werden.

Die Gleichgewichtseinstellung erfolgt nur langsam. Wie Vorversuche zeigten, war sie jedoch nach 8 Stunden auf alle Fälle beendet. Nach Erreichen des Gleichgewichtes wurde der Hahn D geschlossen, der Dampf durch den Hahn B in eine evakuierte, tiefgekühlte Kühlspirale abgesogen und ausgefroren. Der Inhalt der Kühlspirale

* Nähere Angaben über die verwendete Apparatur sowie über die Versuchsergebnisse finden sich bei G. Dändliker, Diss. E. T. H. Zürich, 1955.

gibt die Zusammensetzung der Dampfphase, während die Untersuchung der flüssigen Phase durch Probeentnahme aus dem Kölbchen K erfolgt. Die Analyse wurde refraktometrisch durchgeführt.

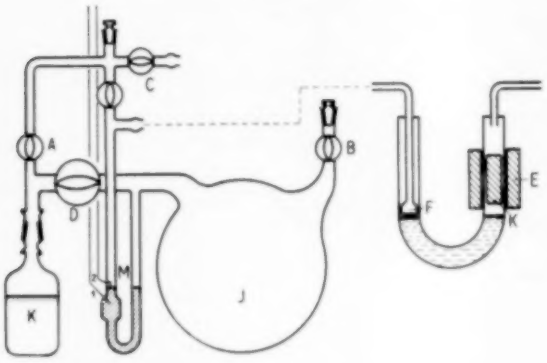

Fig. 1. Statische Apparatur.

b. Substanzen.

Es wurde Pyridin "pro analysi" Merck verwendet, das über Kalk sorgfältig destilliert wurde ($n^{21}{}_D = 1{\cdot}50954$). Die Destillation in einer Podbielniak-Kolonne mit ca. 150 theoretischen Böden ergab keine Aenderung des Brechungsindex. Die Prüfung mittels Karl Fischer-Reagenz lieferte einen Wassergehalt von weniger als 0·1 Mol%.

3. Ergebnisse der Dampfdruckmessungen

Die bei 30° und 50° mit der statischen Apparatur erhaltenen Ergebnisse sind in den Tabellen 1 und 2 zusammengefasst. Die Partialdrucke wurden aus den Gleichungen

$$p_1 = yP \text{ und } p_2 = (1 - y)\,P$$

erhalten. Die Aktivitätskoeffizienten wurden berechnet nach den Beziehungen*

$$\gamma_1 = \frac{yP}{xp^0{}_1} \text{ und } \gamma_2 = \frac{(1 - y)\,P}{(1 - x)\,p^0{}_2}$$

Die Ergebnisse der statischen Methode sind für 50° in Fig. 2 mit den Resultaten der dynamischen Methode verglichen. Die Uebereinstimmung ist befriedigend. Die ausgezogenen Linien sind thermodynamisch widerspruchsfrei und genügen der Gibbs-Duhem'schen Gleichung.

* Die verwendeten Formelzeichen sind am Ende der Arbeit zusammengefasst.

Tabelle 1.

$100\,x$	$100\,y$	$P\,(mm)$	$p_1\,(mm)$	$p_2\,(mm)$	γ_1	γ_2
0·0	0·0	72·1	—	72·1	—	1·000
9·8	23·9	86·0	20·6	65·4	2·27	1·005
10·4	24·0	86·1	20·7	65·4	2·15	1·012
18·6	34·9	93·5	32·6	60·9	1·89	1·038
27·7	46·1	102·1	47·1	55·0	1·84	1·055
32·4	49·7	104·5	51·9	52·6	1·73	1·079
39·1	55·8	107·1	59·8	47·3	1·65	1·077
40·3	56·6	108·4	61·3	47·1	1·65	1·093
48·1	60·6	111·2	67·4	43·8	1·51	1·171
60·4	68·2	115·0	78·4	36·6	1·40	1·28
71·2	73·0	115·4	84·2	31·2	1·28	1·50
82·6	76·6	114·5	87·7	26·8	1·148	2·14
93·0	79·6	113·1	90·0	23·1	1·045	4·57
99·0	88·6	104·3	92·4	11·9	1·009	16·5
100·0	100·0	92·5	92·5	—	1·000	—

Ergebnisse der statischen Messungen bei 50°C.

Tabelle 2.

$100\,x$	$100\,y$	$P\,(mm)$	$p_1\,(mm)$	$p_2\,(mm)$	γ_1	γ_2
0·0	0·0	27·0	—	27·0	—	1·000
6·6	16·2	30·2	4·9	25·3	2·33	1·003
15·0	30·1	32·9	9·9	23·0	2·08	1·002
23·7	37·7	34·7	13·1	2, 6	1·74	1·048
36·1	—	36·8	—	—	—	—
51·0	—	38·4	—	—	—	—
58·7	64·9	39·1	25·4	13·7	1·36	1·23
71·3	73·2	40·0	29·3	10·7	1·29	1·38
74·7	74·5	40·0	29·8	10·2	1·25	1·49
81·3	76·9	39·8	30·6	9·2	1·18	1·82
91·0	79·9	38·7	30·9	7·8	1·068	3·20
92·2	80·4	38·6	31·0	7·6	1·057	3·60
100·0	100·0	31·8	31·8	—	1·000	—

Ergebnisse der statischen Messungen bei 30°C.

Die p_1-Kurve wurde aus der p_2- Kurve erhalten durch graphische Integration der Gleichung[10]

$$\left|\ln \gamma_1\right|_{x_1}^{x_2} = -\int_{x_1}^{x_2} \frac{1 - x}{x}\, d \ln \gamma_2$$

In Fig. 3 werden die bei 30° ermittelten Werte mit jenen von Ewert[2] verglichen. Während die Gesamtdrucke angenähert übereinstimmen, sind die Abweichungen bei den Partialdrucken

VOL. 5 1956

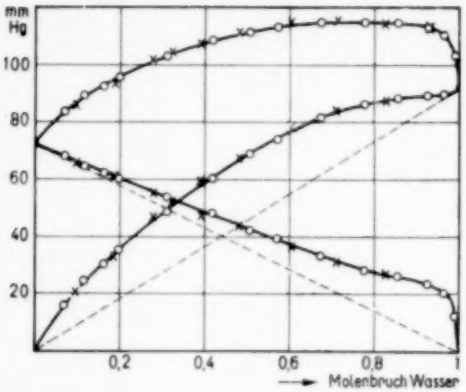

Fig. 2. Dampfdruckdiagramm des Systems Wasser-Pyridin bei 50°C.
O Dynamische Methode
X Statische Methode

zum Teil erheblich. Dies dürfte damit zusammenhängen, dass Ewert die Partialdrucke nicht gemessen, sondern nach einem Integralansatz aus dem Gesamtdruck errechnet hat.

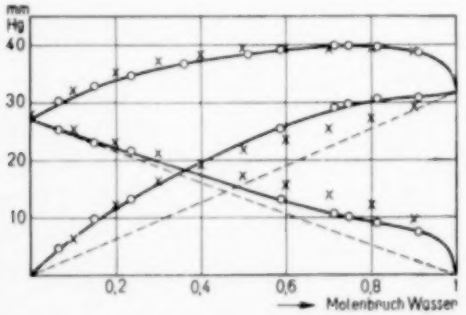

Fig. 3. Dampfdruckdiagramm des Systems Wasser-Pyridin bei 30°C.
O Werte dieser Arbeit (statisch)
X Werte nach Ewert

Mit steigender Temperatur nehmen die Aktivitätskoeffizienten zu, d.h. dass die Abweichungen vom idealen Verhalten grösser werden, während bei den meisten binären Gemischen das entgegengesetzte Verhalten beobachtet wird. Die Zunahme von γ ist allerdings ziemlich gering, wie Fig. 4, in der die Aktivitätskoeffizienten für 30, 50 und 80°* eingetragen sind, zu entnehmen ist.

* Die für 80° verwendeten Aktivitätskoeffizienten sind einer früheren Arbeit entnommen[6].

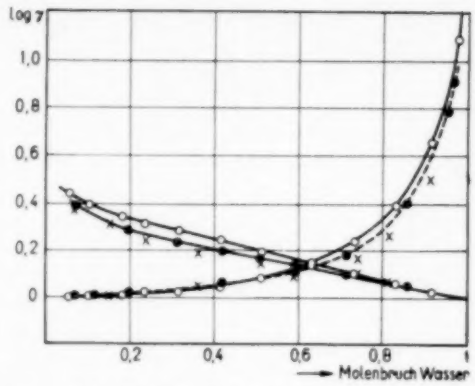

Fig. 4. Die Aktivitätskoeffizienten bei verschiedenen Temperaturen.
– O – Werte bei 80° (dynam.)
– ● – Werte bei 50° (dynam.)
– X – Werte bei 30° (stat.)

Aus der Temperaturabhängigkeit des Aktivitätskoeffizienten kann die differentielle Lösungswärme ΔH_2 des Pyridins berechnet werden nach der Beziehung[11a]

$$\Delta H_2 = - RT^2 \left[\frac{\partial \ln \gamma_2}{\partial T}\right]_x$$

Für $x = 0{\cdot}8$ erhält man zwischen 50° und 80° $-0{\cdot}8$ kcal/Mol und zwischen 30° und 50° $-1{\cdot}0$ kcal/Mol. Diese Werte können mit den kalorimetrischen Messungen von Baud[12] verglichen werden. Aus den von diesem Autor angegebenen Mischungswärmen ergibt sich für $x = 0{\cdot}8$ und 13°C ein ΔH_2 – Wert von $-1{\cdot}25$ kcal/Mol (berechnet nach der Methode des Ordinatenabschnittes der Tangente, vergl. z.B. Kortüm[11b]). Anderseits haben neuerdings Andon, Cox und Herington[4,7], aus den von ihnen gemessenen Aktivitätskoeffizienten für die differentielle Lösungswärme des Pyridins bei unendlicher Verdünnung zwischen 70 und 100° einen Wert von $-0{\cdot}3$ kcal/Mol, zwischen 25 und 40° einen solchen von $-2{\cdot}0$ kcal/Mol errechnet.

4. Das Azeotrop

Die von verschiedenen Autoren erhaltenen Zusammensetzungen des azeotropen Gemisches sind in Tabelle 3 zusammengestellt. Neuerdings

hat Fowler[9] das Azeotrop des Systems Wasser-Pyridin näher untersucht und dabei eine ziemlich ausgeprägte Abhängigkeit der Zusammensetzung von der Temperatur festgestellt. In der vorliegenden Arbeit wurde dagegen nur eine sehr geringe Verschiebung des azeotropen Punktes gefunden, die praktisch innerhalb der Fehlergrenze lag (vergl. Tabelle 4). Dieses Ergebnis stimmt mit demjenigen von Jones und Speakman[13] überein (vergl. auch Hisamura u. Mitarb[14].)

Tabelle 3.

Temp. (°C)	*Zusammensetzung Mol* % H_2O	*Autor*
92–93	77·5	Goldschmidt u. Costam[15]
94·0	76·7	Baud[12]
80·0	75·2	Zawidzki[1]
64·2–93·0	76·0	Jones u. Speakman[13]
92·6	77·0	Lecat[16]
49·3	79·0	Fowler[3]
83·0	76·0	Fowler[3]
94·4	76·7	Vriens und Medcalf[5]
94·4	75·75	Wagner[8]
30·0–80·0	74–75	Diese Arbeit.

Zusammensetzung des Azeotrops nach verschiedenen Autoren.

Tabelle 4.

Temp. (°C)	*Zusammensetzung Mol* % H_2O	*Methode*
30	74·3	statisch
50	74·3	statisch
50	73·9	dynamisch
60	74·2	dynamisch
80	75·0	dynamisch

Temperaturabhängigkeit des Azeotrops nach den Versuchen dieser Arbeit.

Die weitgehende Konstanz der azeotropen Zusammensetzung, sowie die Tatsache, dass letztere etwa 1 Mol Pyridin auf 3 Mole Wasser beträgt, ist im älteren Schrifttum (so namentlich von Goldschmidt und Constam[15]) auf das Vorhandensein einer definierten Verbindung der Formel $C_5H_5N{\cdot}3H_2O$ zurückgeführt worden. Auch Baud[12] hat aus seinen Dampfdichtemessungen auf eine zumindest teilweise Komplexbildung in der Dampfphase geschlossen. Die Frage der Existenz einer definierten Verbindung ist u.a. von Bedeutung im Hinblick auf die Prüfung der Messwerte auf thermodynamische Konsistenz mittels der Gibbs-Duhem'schen Gleichung. Für die Gültigkeit dieser Beziehung spielt eine allfällige Komplexbildung in der flüssigen Phase keine Rolle; falls jedoch eine Verbindung in der Gasphase vorhanden ist, kann die Gibbs-Duhem'sche Gleichung nicht mehr in der üblichen Weise angewendet werden. In der vorliegenden Arbeit wurde deshalb die Dampfdichte des azeotropen Gemisches nach der Methode von Hofmann zwischen 60 und 80° erneut geprüft, wobei im Einklang mit den Messungen von Jones und Speakman[13] normale Molekulargewichte (MG) gefunden wurden*. So ergaben z.B. 3 Messungen bei 80° und bei 0·215, 0·185 und 0·096 at MG-Werte von 33·5, 33·4 und 33·5 gegenüber einem Wert von 33·6 für den Fall der vollständigen Dissoziation in Pyridin und Wasser (MG des hypothetischen Hydrats: 133).

* Diplomarbeiten E. T. H. von HOIGNÉ (1954) und MANUKIAN (1955).

VERWENDETE FORMELZEICHEN

x = Molenbruch des Wassers in der flüssigen Phase.
y = Molenbruch des Wassers in der Dampfphase.
P = Gesamtdruck.
p_1 = Partialdruck des Wassers.
p_2 = Partialdruck des Pyridins.
p^0_1 = Dampfdruck des reinen Wassers.
p^0_2 = Dampfdruck des reinen Pyridins.
γ_1 = Aktivitätskoeffizient des Wassers.
γ_2 = Aktivitätskoeffizient des Pyridins.
T = Absolute Temperatur.
R = Ideale Gaskonstante.

LITERATUR

[1] ZAWIDZKI, J. VON ; *Z. physik. Chem.* 1900 **35** 196.

[2] EWERT, M. ; *Bull. Soc. chim. Belges* 1936 **45** 493.

[3] FOWLER, R. T. ; *J. Appl. Chem.* (London) 1952 **2** 246

[4] ANDON, R. J. L., COX, J. D., HERINGTON, E. F. G. ; Discussions Faraday Soc. 1953 **15** 168.

[5] VRIENS, G. N., MEDCALF, E. C. ; *Ind. Eng. Chem.* 1953 **45** 1098.

[6] IBL, N., DÄNDLIKER, G., TRÜMPLER, G. ; *Helv. Chim. Acta.* 1954 **37** 1661.

[7] ANDON, R. J. L., COX, J. D., HERINGTON, E. F. G. ; *J. Chem. Soc.* 1954 3188

[8] WAGNER, R. E. ; Ph.D.Thesis in Chemical Engineering, Princeton University 1952.

[9] KORTÜM, G., MOEGLING, D., WOERNER F. ; *Chem. Ing. Tech.* 1950 **22** 453.

[10] DODGE, B. F. ; Chemical Engineering Thermodynamics (McGraw Hill 1944), 5.562.

[11] KORTÜM, G. und BUCHHOLZ-MEISENHEIMER, H. ; Die Theorie der Destillation und Extraktion von Flüssigkeiten (SPRINGER, 1952), (a) S.93, (b) S.17-18.

[12] BAUD, E. ; *Bull. Soc. Chim. France* (4) 1909 **5** 1022.

[13] JONES, W. J., SPEAKMAN, J. B. ; *J. Am. Chem. Soc.* 1921 **43** 1867.

[14] HISAMURA, M., OKAZAKI, T., MATSUYAMA, A. ; *Coal Tar* (Japan) 1950 **2** 132. C.A. 1952 **46** 7837$_e$.

[15] GOLDSCHMIDT, H., CONSTAM, E. J. ; *Ber.* 1883 **16** 2976.

[16] LECAT, M., *Ann. Soc. Sci. Bruxelles*, Sér. I. 1947, **61** 73.

VOL.
5
1956

Book reviews

K. G. Denbigh: The Principles of Chemical Equilibrium, Cambridge University Press, 1955. 491 pp., numerous tables, 42s.

The author of *The Principles of Chemical Equilibrium* is known the world over as author of a monograph *The Thermodynamics of the Steady State*. This little book was notable as a relatively successful attempt at an operational approach to a difficult subject, namely, the application of the Onsager reciprocal relations to irreversible coupled flows. In the present volume Professor Denbigh has undertaken a task less ambitious in principle and more ambitious in scope. It does not include the subject of his other work.

Formerly University Lecturer in the Department of Chemical Engineering at Cambridge University, Professor Denbigh has recently become Professor of Chemical Technology at the University of Edinburgh and Professor of Chemical Engineering at the Heriot-Watt College. He has lectured at many universities in the United States.

In the preface the author remarks that his book is intended not for the beginner in thermodynamics, but for the student who is on his second or third round. He proposes that the student should go over again the basis of the first and second laws, but "this time in a more logical sequence." A generous collection of graded problems, including some from the qualifying and final examinations for the Cambridge University Chemical Engineering degree, appears at the end of each chapter.

The Table of Contents lists the heading of each Part, Chapter, and Section. Then comes a list of symbols with an indication of the page and equation where the definition of the quantity symbolized is to be found. Next is a Table of Values of Physical Constants.

The book is subdivided into three parts. Part I, "The Principles of Thermodynamics," consists of the following chapters: First and Second Laws, Auxiliary Functions and Conditions of Equilibrium. Part II, "Reaction and Phase Equilibria," consists of the following: Thermodynamics of Gases, Equilibria of Reactions Involving Gases, Phase Rule, New Phase Equilibria in Single Component Systems, General Properties of Solutions and the Gibbs-Duhem Equation, Ideal Solutions, Non-Ideal Solutions, Reaction Equilibrium in Solution, Electrolytes. Part III, "Thermodynamics in Relation to the Existence of Molecules," consisting of the following: Statistical Analogues of Entropy and Free Energy, Partition Function of a Perfect Gas, Perfect Crystals and the Third Law, Regular Solutions and Absorption, Chemical Equilibrium in Relation to Chemical Kinetics, The Transition State Theory.

An appendix entitled "Answers to Problems and Comments" outlines the solutions to many of the more difficult problems. An adequate index completes the book.

Three things are essential to a good textbook in thermodynamics: logical consistency, logical completeness, and good taste. Taste enters because choices may be made in the selection of axioms. The choice that is made reflects oftentimes the training, prejudices, predilections, and even the æsthetic qualities of the author. The logical qualities can be judged objectively, but any judgement of taste must, of course, reflect the taste of the critic.

This book is devoted primarily to the macroscopic or phenomenological treatment of states and processes. Part III, however, is the microscopic treatment; and the author's competence in exposition of molecular phenomena colours inevitably his exposition of the macroscopic. For example, on page 15 reference is made to the difference between the "internal pressure" of a gas and the external force per unit area in a rapid change of volume. Here the internal pressure must be a microscopic concept. Perhaps the same question is involved on page 23, where "the pressure acting on the piston" is distinguished from "the pressure of the fluid itself," and on page 45. On page 119 it is stated that expansion of a gas "always leads to a cooling, on account of the decrease in internal energy consequent on the performance of work." From the standpoint of thermodynamics this is a dangerous half truth. For water below the temperature of maximum density this is not true – and in what macroscopic sense does this water differ from gaseous water?

Notwithstanding these critical comments, the reviewer was favourably impressed with the author's exposition of thermodynamics as a macroscopic science. The procedure is to define equality of temperature and adiabatic wall, to state the zeroth law, to introduce work, and then to state the first law in the manner of Caratheodory, namely, that work in adiabatic processes is fixed by the end states. Heat is then defined as the difference between change of energy (adiabatic work) and work, and the connection is made with calorimetric heat.

The statement on page 14 that "the notion of work is not regarded as being in need of definition in thermodynamics, since it is a concept which is already defined by the primary science of mechanics" is unfortunately not well founded. In the science of mechanics work is almost never defined as an interaction between systems, which it must be in thermodynamics.

The statement of the second law is adequate, though lacking in conciseness. The proof that entropy is a property is based on the substitution of constant-entropy, constant-temperature steps for the elements of a continuous cyclic process. This method seems to restrict the validity of the result to systems in which all temperature changes can be brought about reversibly and adiabatically. The more general approach is implied in the footnote of page 37.

It is good to find on page 41 the statement that if an

VOL. 5 1956

exchange of matter occurs between two bodies the notion of heat flow at the point of exchange becomes ambiguous, although energy flow may still be defined. This is, of course, a basic consideration in coupled irreversible flows.

The statement that $dS = dq/T$ is " applicable to processes of pure heat transfer, even when they are not carried out under reversible conditions, provided that the temperature remains sensibly uniform . . ." is likely to give trouble to the student. Heat transfer always involves irreversibility in some order of magnitude. A discussion of relative orders and their effects on the applicability of the equation $dS = dq/T$ would be better than remarking on an exception to the reversibility requirement.

The troublesome relation $dU = TdS - pdV$ is discussed a number of times quite well, but never with the clarity that is needed. In the derivation and statement of the steady-flow energy equation, the student is warned against transfer of his conservation principle from energy to enthalpy. The statements of maximum work in terms of the decrease in the Gibbs free energy is generalized from the usual restriction of constancy of temperature and pressure to a change between states of the same temperature and pressure. These are important things that are omitted in many good textbooks.

A difficult subject for the student of chemical equilibrium is the identification of components, as distinguished from species. This subject is treated competently on pages 169 and 185. It should have been introduced on page 75 in connection with equation (2.38) which is clearly in terms of components.

The term " fundamental equation," is generally reserved for the equation which expresses a property in terms of a characteristic function in the sense employed by Massieu. The author uses the term in this sense on page 78, but in a different sense four pages earlier.

The symbols and nomenclature will be familiar to American students. The student of engineering will be glad to find that upper and lower cases are used to distinguish between total and specific (per unit mass or per mole) values of extensive properties, a practice which has not been adopted by chemists. Some minor difficulties which have not been resolved in America are not resolved here. For example F in the lower case represents both free energy per mole and fugacity. An even less happy choice of symbols appears on pages 444 and 445, where the different kinds of β's and γ's are confusing.

The exposition of equilibrium of mixtures and solutions is necessarily plagued with the variety of standard states (states of unit activity) and reference states (states of unit activity coefficient). Here the treatment is orderly and as simple as may be. Perfect-gas mixtures and ideal solutions are defined by analogous statements. The standard states for the non-perfect or non-ideal are chosen at the pressure and temperature of the system. The author says that in some American texts the standard state is at unit pressure. The practice in some of the best American texts, however, is in accord with the author's. The standard state of an un-ionized salt of a strong electrolyte is not discussed.

The number of helpful comments and discussions of practical considerations is impressive. Many of these are in the form of footnotes and the number of footnotes is unusually large. It seems that many footnotes are so good and so germane to the exposition that they could well have been included in the text. The author's general comments and discussion of experimental aspects are often very enlightening. The following are a few examples : reversible combustion of carbon on page 71 ; comparison of the equilibrium criteria in terms of free energy and entropy for a system, and a system and its isothermal environment on page 82 ; the equilibrium constant expressed in terms of different properties (molality, mole fraction, and vapour pressure) for different species on pages 292 and 293 ; second-order transitions, beginning on page 205 ; and microscopic reversibility on page 446.

The reviewer's general impression is that this is an easy book to read. Compared with other good books on the subject it is more limited in the range of thermodynamic material covered, although it offers a bonus, seldom found in the others, in its Part III. The material covered is sufficient for most graduate study, because it is the concepts which are hardest to teach and these are well presented. The book will appeal to engineers because its author thinks like an engineer. Its soundness should recommend it to scientists as well. It will probably find a good market in America, where its orderliness and clarity will be appreciated.

Joseph H. Keenan

C. P. Smyth : **Dielectric Behaviour and Structure,** McGraw-Hill Book Company, Inc., New York, 1955. 441 pp., $9.00.

This is a completely rewritten version of the author's earlier work entitled *Dielectric Constant and Molecular Structure*. The new book deals particularly with the relations between dielectric loss and dielectric constant on the one hand, and molecular structure and intermolecular forces on the other.

The first half of the book is concerned with theories of dielectric behaviour, and with interpretation of the data in terms of molecular structure. There is also a rather short discussion on high polymers – a section which, in the opinion of the reviewer, might well have been extended to deal in detail with polythene and also with Teflon (polytetrafluoroethylene). This half of the book concludes with a chapter on the experimental determination of dielectric constants and losses.

The second half of the book is concerned with the detailed use of dipole moment measurements in determining molecular structure, and in the study of resonance and intramolecular energies.

This is undoubtedly a book to which every chemical engineer should have access. The type and illustrations are clear, and there are many recent references. In a

subject which has grown very rapidly in recent years, we must be grateful for even a short section on microwave techniques and results. Chemical engineers, however, may regret the omission of several interesting fields, particularly the influence of molecular orientation in membranes on dielectric constant, (K. S. Cole), dielectric constants at interfaces, and the dielectric behaviour of gases absorbed on powders (e.g. McIntosh, Rideal and Snelgrove, 1951).

However, the book as it stands is a valuable survey and summary of the literature, and is also readable enough to serve as an introduction to the subject. We should be grateful to Dr. Smyth for presenting us with another authoritative work on molecular structure and dielectrics, for in this union lies the possibility of preparing new insulators of any special properties we may require.

J. T. Davies

F. A. Henglein: **Grundriss Der Chemischen Technik.** Verlag Chemie. GMBH. Weinheim/Bergstrasse, 1954. 762 pp., DM. 49.80.

This is a descriptive compendium of the methods, equipment, and practices of the chemical process industries and, because it covers such a wide variety of topics, it is necessarily brief in its treatment of each. Only elementary theory is introduced, so that it is the "how" rather than the "why" of the industrial chemical field which is presented. Subjects touched upon range from patent classification to plant layout, and from leather manufacture to process history. Much care has been taken in selecting the many illustrations, flow sheets, etc. The book will not appeal to the specialist, nor to the student of quantitative chemical engineering, but rather it will serve as a one-volume encyclopaedic reference to industrial practice in the process industries. Edgar L. Piret

VOL.
5
1956

Editorial Announcement

In response to the large number of papers submitted to the Journal, the editors and publishers are happy to announce that it will in future be published every month instead of every two months. The increased rate of publication will make it possible to reduce very greatly the time-lag between acceptance and publication of manuscripts.

It is hoped to publish, in future, two volumes a year.